Sampling and misspecification errors in the estimation of observation-error covariance matrices using observation-minus-background and observation-minus-analysis statistics

Received: 11 November 2022 | Revised: 21 February 2024 | Accepted: 10 April 2024

DOI: 10.1002/qj.4750

Quarterly Journal of the Royal Meteorological Society RMetS

RESEARCH ARTICLE

Sampling and misspecification errors in the estimation of observation-error covariance matrices using observation-minus-background and observation-minus-analysis statistics

Guannan Hu[1,2] | **Sarah L. Dance**[1,2,3]

[1]Department of Meteorology, University of Reading, Reading, UK

[2]National Centre for Earth Observation (NCEO), University of Reading, Reading, UK

[3]Department of Mathematics and Statistics, University of Reading, Reading, UK

Correspondence
Guannan Hu, Department of Meteorology, University of Reading, Reading, UK.
Email: guannan.hu@reading.ac.uk

Funding information
Natural Environment Research Council; Engineering and Physical Sciences Research Council, UK EPSRC DARE project, Grant/Award Number: EP/P002331/1; Met Office

Abstract

Specification of the observation-error covariance matrix for data assimilation systems affects the observation information content retained by the analysis, particularly for observations known to have correlated observation errors (e.g., geostationary satellite and Doppler radar data). A widely adopted approach for estimating observation-error covariance matrices uses observation-minus-background and observation-minus-analysis residuals, which are routinely produced by most data assimilation systems. Although this approach is known to produce biased and noisy estimates, due to sampling and misspecification errors, there has been no systematic study of sampling errors with this approach to date. Furthermore, the eigenspectrum of the estimated observation-error covariance matrix is known to influence the analysis information content and numerical convergence of variational assimilation schemes. In this work, we provide new theorems for the sampling error and eigenvalues of the estimated observation-error covariance matrices with this approach. We also conduct numerical experiments to illustrate our theoretical results. We find that this method produces large sampling errors if the true observation-error standard deviation is large, while the other error characteristics, including the true background-error standard deviation and observation- and background-error correlation length-scales, have a relatively small effect. We also find that the smallest eigenvalues of the estimated matrices may be smaller or larger than the true eigenvalues, depending on the assumed and true observation- and background-error statistics. These results may provide insights for practical applications: for example, in deciding on appropriate sample sizes and choosing parameters for matrix reconditioning techniques.

KEYWORDS

correlated observation errors, data assimilation, Desroziers et al. diagnostic, misspecification error, observation-error covariance matrix, sampling error

1 | INTRODUCTION

Data assimilation is a technique used in numerical weather prediction (NWP) to provide initial conditions for weather forecasting models. Such models are sensitive to initial conditions and therefore we should provide initial conditions that are as close to the true atmospheric state as possible (e.g., Dance *et al.*, 2019; Hu *et al.*, 2022). These initial conditions are referred to as *analyses* in data assimilation systems and are created using short-range model forecasts, observational data, and their error statistics.

Observation-error covariance matrices are used in data assimilation to take account of the observation uncertainty. How well the observation-error covariance matrices represent the true error statistics affects the results of the data assimilation and hence the quality of any subsequent weather forecasts. In some practical NWP applications, observation errors are assumed to be uncorrelated and so the observation-error covariance matrices are diagonal. The assumption of uncorrelated observation errors is a pragmatic strategy when we do not have a good understanding of the characteristics of observation uncertainty (e.g., Liu & Rabier, 2003). Observation-error correlations can be accounted for indirectly by artificially enlarging the observation-error variance. However, this is suboptimal and results in reduced analysis accuracy compared with including observation-error correlations explicitly (Stewart *et al.*, 2008, 2013; Weston *et al.*, 2014). Spatial error correlations can be removed by observation thinning, but this prevents us from making full use of the information from high-resolution observations (e.g., Cordoba *et al.*, 2017; Fowler *et al.*, 2018; Rainwater *et al.*, 2015; Waller *et al.*, 2016c). Many studies show that, when assimilating observations that are known to have correlated observation errors, there are significant benefits in explicitly including the correlated observation-error statistics in the observation-error covariance matrix by using a non-diagonal matrix (e.g., Bédard & Buehner, 2020; Fujita *et al.*, 2020; Healy & White, 2005; Simonin *et al.*, 2019; Stewart *et al.*, 2008, 2013; Weston *et al.*, 2014). The inclusion of spatially correlated observation-error statistics in data assimilation systems increases the computational cost of matrix inversion, matrix–vector multiplication, and communication costs in parallel computations. This computational issue can be addressed by, for example, adopting a pragmatic strategy for the distribution of observations between processors (Simonin *et al.*, 2019) and using numerical approximation techniques (e.g., Guillet *et al.*, 2019; Hu & Dance, 2021; Michel, 2018).

A number of methods have been developed to estimate correlated observation-error statistics in practical applications (see the reviews by Janjić *et al.*, 2018; Tandeo *et al.*, 2020; Satterfield *et al.*, 2022). A popular approach is to use diagnostics based on the observation-minus-background (O−B) and observation-minus-analysis (O−A) statistics derived by Desroziers *et al.* (2005). These statistics can be easily obtained from a data assimilation system with almost no additional cost. We refer to this approach as the Desroziers et al. method, which is essentially a sampling approach that uses finite samples of the O−B and O−A differences to estimate observation-error covariance matrices. The Desroziers et al. method has been successfully used in operational data assimilation systems to estimate spatial error correlations for observations such as geostationary satellite observations (e.g., Michel, 2018; Waller *et al.*, 2016a) and Doppler radial winds (e.g., Waller *et al.*, 2016c, 2019; Yeh *et al.*, 2022), and to estimate satellite interchannel error covariances (e.g., Bormann *et al.*, 2016; Campbell *et al.*, 2017; Stewart *et al.*, 2014; Weston *et al.*, 2014).

Despite the successful operational use of diagnosed observation-error covariance matrices obtained using this approach, there have only been limited theoretical and applied studies into the accuracy of the observation-error covariance estimates obtained. Waller *et al.* (2017) studied the use of the diagnostic for ensemble assimilation and found that it is only appropriate to apply the diagnostic to certain subsets of observations, depending on the choice of domain localization length. Waller *et al.* (2016b), Ménard (2016), and Bathmann (2018) carried out theoretical studies for variational assimilation methods (with no sampling error) and found that the diagnosed estimates are highly dependent on the background- and observation-error covariances *assumed* in the data assimilation system. The assumed error statistics refer to those used in the assimilation system, which are approximations of the true error statistics. Nevertheless, empirical metrological studies by Chun *et al.* (2015) and Mirza *et al.* (2021) have found good qualitative and quantitative agreement with diagnosed estimates, respectively. None of these studies has considered the effects of statistical sampling error on the diagnosed estimates, although noisy estimates have been observed (Waller *et al.*, 2019). For estimation of covariance matrices using direct sampling, Ledoit and Wolf (2004) found that the sampling error is larger if the ratio of the number of observations to the sample size is larger. In this article, we will demonstrate that this ratio (number of observations/sample size) is also an important factor in controlling the size of the sampling error with the Desroziers et al. method. Previous studies estimating the observation-error covariance matrices using the Desroziers et al. approach show quite a wide variation for this ratio, often for practical reasons. For example, in experiments estimating spatial correlations for Doppler radar winds, the maximum possible number

of observations in a scan is 1920 and the correlation coefficients are estimated using a sample size larger than 500 (Waller *et al.*, 2016c), giving a maximum ratio of number of observations/sample size of 3.8. For satellite interchannel error correlation estimation, these ratios are typically much smaller (Stewart *et al.*, 2014 use ratios between 0.007 and 0.07).

There are numerous studies on the use of sample covariance matrices to estimate large-dimensional covariance matrices (e.g., Dey & Srinivasan, 1985; Haff, 1980; Ledoit & Wolf, 2004). However, most of the literature uses direct sampling methods, in which the sample represents the statistics of the covariance matrix to be estimated. In contrast, the Desroziers et al. method is an indirect sampling method, where assimilation residuals in observation space (not observation errors) are sampled and used to estimate the observation-error covariance matrices. In practice, the sample covariance matrix is often regularised to ensure a better estimate (Bickel & Levina, 2008; Furrer & Bengtsson, 2007). Common methods for covariance regularization in data assimilation include localization for the background-error covariance matrix (e.g., Hamill *et al.*, 2001; Houtekamer & Mitchell, 2001) and ridge regression (RR) and the minimum eigenvalue (ME) method for the observation-error covariance matrix (e.g., Tabeart *et al.*, 2020b). In this work, we investigate the raw sample observation-error covariance (before regularization), as the nature of the sampling errors can help inform the choice of localization method. It should also be noted that, in operational applications with spatially correlated observation errors, the covariance has been estimated by fitting the samples to a specified form of correlation function (Simonin *et al.*, 2019). In this case, additional matrix regularization has not been needed.

In this work, we provide some novel adaptions of Ledoit and Wolf's (2004) theorems on direct sampling errors to give theorems on indirect sampling errors. We investigate how sampling errors grow as the ratio of the number of observations to sample size, observation, and background-error standard deviations and correlation length-scales changes. We also examine the eigenvalues of the estimated observation-error covariance matrices, since the smallest eigenvalues of these matrices were found to affect the speed of convergence of the least-squared minimisation in variational data assimilation (e.g., Tabeart *et al.*, 2018, 2021; Weston *et al.*, 2014). Very small minimum eigenvalues may increase the number of iterations required for convergence. In addition, when assimilating satellite observations, small interchannel biases can be amplified by very small eigenvalues (Geer, 2019). Previous work has shown that modifying the eigenvalues of the observation-error covariance matrices by using matrix reconditioning techniques, such as ME and RR methods, can improve the condition number of the matrix (e.g., Tabeart *et al.*, 2020b) and convergence speed of the variational minimization (e.g., Tabeart *et al.*, 2020a). Our investigation on sample eigenvalues may provide some guidance on how to choose the parameters of these reconditioning methods for practical applications.

We organise our article as follows. In Section 2, we introduce some key mathematical concepts that will be used later in our analysis of sampling error, including eigenvalue value decomposition, the Frobenius norm, and the matrix trace. In Section 3, we introduce the notation and terminology of data assimilation. In Section 4, we describe how to use the Desroziers et al. method to estimate observation-error covariance matrices. In Section 5, we present previous work on sampling error with a direct sampling approach, which will be used in our analysis of sampling error with the Desroziers et al. method. In Section 6, we show our new theoretical results on sampling error with the Desroziers et al. method. In Section 7, we examine how well the true eigenvalues of the observation-error covariance matrices are approximated by those of the estimated matrices. In Section 8, we conduct a number of numerical experiments to illustrate our theoretical analysis. Finally, in Section 9, we summarise our work and discuss how our findings may provide useful information for practical applications of the Desroziers et al. method.

2 | MATHEMATICAL PRELIMINARIES

In this section, we introduce some key mathematical concepts and notation that are used in this study.

2.1 | Eigendecomposition

Eigendecomposition factorises a diagonalizable matrix into eigenvalues and eigenvectors (e.g., Golub & Van Loan, 1996, chapter 8). The eigenvalues obtained will be used later in our analyses of sampling errors (Sections 5 and 6). In addition, we are interested in the eigenvalues of the observation-error covariance matrices, because the smallest eigenvalue is considered to be a key factor affecting the numerical convergence of variational data assimilation methods (e.g., Tabeart *et al.*, 2018, 2021). New results on eigenvalues are discussed in Section 7.

Let $\mathbf{A} \in \mathbb{R}^{m\times m}$ be any covariance matrix, which is symmetric and positive semi-definite by definition. It can be decomposed as

$$\mathbf{A} = \mathbf{U}\boldsymbol{\Lambda}\mathbf{U}^{\top}, \tag{1}$$

where $\mathbf{\Lambda} \in \mathbb{R}^{m\times m}$ is a diagonal matrix with diagonal elements that are the eigenvalues $\lambda_1(\mathbf{A}) \geq \lambda_2(\mathbf{A}) \geq \ldots \geq \lambda_m(\mathbf{A})$, and $\mathbf{U} \in \mathbb{R}^{m\times m}$ is a matrix with columns that are the corresponding eigenvectors $\mathbf{u}_1, \mathbf{u}_2, \ldots, \mathbf{u}_m$. The eigenvectors are orthonormal, that is, $\mathbf{U}^{\mathsf{T}}\mathbf{U} = \mathbf{I}$.

2.2 | The Frobenius norm, Frobenius inner product, and matrix trace

The *Frobenius norm* is defined as the square root of the sum of the absolute squares of the matrix elements (e.g., Bernstein, 2009, chapter 9),

$$\|\mathbf{A}\|_{\mathrm{F}} = \sqrt{\sum_{i=1}^{m}\sum_{j=1}^{m}|a_{i,j}|^2}, \tag{2}$$

where $a_{i,j}$ denotes the element in the ith row and jth column of $\mathbf{A}$. The Frobenius norm will be used later to measure the elementwise difference between the true and sample covariance matrices. The Frobenius norm provides a standard way to measure the difference between two matrices and is easier to compute than the matrix norms induced by vector p-norms (e.g., Golub & Van Loan, 1996, chapter 2). Furthermore, our work builds on the work of Ledoit and Wolf (2004), and their calculations depend on the properties of the Frobenius norm (e.g., Bernstein, 2009, chapter 9), but it would be straightforward to extend them to a weighted Frobenius norm (Higham, 2002).

We also need to introduce the *Frobenius inner product*, which is defined as the sum of entries of the Hadamard product for real-valued matrices,

$$\langle \mathbf{A}_1, \mathbf{A}_2 \rangle_{\mathrm{F}} = \sum_{i,j}^{m} a_{i,j}\widehat{a}_{i,j}, \tag{3}$$

where $\langle \cdot, \cdot \rangle_{\mathrm{F}}$ denotes the Frobenius inner product of any two matrices of the same dimension. The Frobenius inner product will be used in Theorems 1 and 4. Finally, the *trace* of the matrix $\mathbf{A}$ is defined to be the sum of its diagonal entries,

$$\mathrm{tr}(\mathbf{A}) = \sum_{i=1}^{m} a_{i,i}, \tag{4}$$

which is equal to the sum of the eigenvalues

$$\mathrm{tr}(\mathbf{A}) = \sum_{i=1}^{m} \lambda_i(\mathbf{A}). \tag{5}$$

The trace will be used in the definition of a quantity that affects sampling error in Section 5.

3 | SOME BASIC DATA ASSIMILATION CONCEPTS

Data assimilation blends information from observations and short-range model forecasts by taking account of their uncertainties. The symbol $\mathbf{y} \in \mathbb{R}^m$ is used to denote the observation vector and the symbol $\mathbf{x}^{\mathrm{b}} \in \mathbb{R}^n$ is used to denote the vector given by the short-range model forecast, which is referred to as the *background* model state vector. In data assimilation, observation and background errors are typically assumed to be Gaussian-distributed and unbiased. Let $\mathbf{x}^{\mathrm{t}} \in \mathbb{R}^n$ be the true system state, then we may write

$$\mathbf{y} = H(\mathbf{x}^{\mathrm{t}}) + \boldsymbol{\epsilon}^{\mathrm{o}}, \tag{6}$$

where $H : \mathbb{R}^n \to \mathbb{R}^m$ is the nonlinear observation operator and $\boldsymbol{\epsilon}^{\mathrm{o}} \in \mathbb{R}^m$ is a vector containing the observation errors. The observation errors are assumed to follow a Gaussian distribution with zero mean and covariances given by the observation-error covariance matrix, $\mathbf{R} \in \mathbb{R}^{m\times m}$, that is, $\boldsymbol{\epsilon}^{\mathrm{o}} \sim \mathcal{N}(0, \mathbf{R})$. It should be noted that, in Equation (6), the observation operator is not assumed to be perfect. Observation-operator uncertainty is included in the definition of the matrix $\mathbf{R}$ (Janjić *et al.*, 2018). Similar to Equation (6), we have

$$\mathbf{x}^{\mathrm{b}} = \mathbf{x}^{\mathrm{t}} + \boldsymbol{\epsilon}^{\mathrm{b}}, \tag{7}$$

where $\boldsymbol{\epsilon}^{\mathrm{b}} \in \mathbb{R}^n$ is a vector containing the background errors and $\boldsymbol{\epsilon}^{\mathrm{b}} \sim \mathcal{N}(0, \mathbf{B})$. The matrix $\mathbf{B} \in \mathbb{R}^{n\times n}$ is known as the background-error covariance matrix.

The analysis equation is given by for example, Bouttier and Courtier (2002) and Nichols (2010)

$$\mathbf{x}^{\mathrm{a}} = \mathbf{x}^{\mathrm{b}} + \widetilde{\mathbf{K}}\mathbf{d}^{\mathrm{b}}, \tag{8}$$

where $\mathbf{x}^{\mathrm{a}} \in \mathbb{R}^n$ is the analysis state vector, $\widetilde{\mathbf{K}} \in \mathbb{R}^{n\times m}$ the Kalman gain matrix assumed in a data assimilation system, and $\mathbf{d}^{\mathrm{b}} \in \mathbb{R}^m$ the *observation-minus-background* (O−B) residual (defined in Equation (10) below). The assumed Kalman gain matrix is calculated as

$$\widetilde{\mathbf{K}} = \widetilde{\mathbf{B}}\mathbf{H}^{\mathsf{T}}(\mathbf{H}\widetilde{\mathbf{B}}\mathbf{H}^{\mathsf{T}} + \widetilde{\mathbf{R}})^{-1}, \tag{9}$$

where $\widetilde{\mathbf{B}} \in \mathbb{R}^{n\times n}$ and $\widetilde{\mathbf{R}} \in \mathbb{R}^{m\times m}$ are *assumed* background and observation-error covariance matrices, respectively, and $\mathbf{H} \in \mathbb{R}^{m\times n}$ is the observation operator linearised about the current state. We have used a tilde here in order to help distinguish these assumed matrices from the exact statistics. The assumed error covariance matrices are the matrices used in a data assimilation system, which may not be exact, that is, they may not describe the

true error statistics completely correctly. The distinction between the assumed and true error covariance matrices is needed in the analysis of the Desroziers et al. method. The O−B residual is computed as the difference between the observations and background model state in observation space,

$$\mathbf{d}^{\mathrm{b}} = \mathbf{y} - H(\mathbf{x}^{\mathrm{b}}). \tag{10}$$

Another quantity used in the Desroziers et al. method is the *observation-minus-analysis* (O−A) residual, given as the difference between the observations and analysis in observation space,

$$\mathbf{d}^{\mathrm{a}} = \mathbf{y} - H(\mathbf{x}^{\mathrm{a}}). \tag{11}$$

4 | THE ESTIMATION OF OBSERVATION-ERROR COVARIANCE MATRICES

A straightforward way of estimating the true observation-error covariance matrix would be to use samples of observation errors. This approach is described in Section 4.1. However, direct sampling is not always possible in practice. Instead, the Desroziers et al. method is often used, which can be considered as an indirect sampling approach, as it does not use samples of observation errors. The Desroziers et al. approach is described in Section 4.2.

4.1 | Direct estimation of observation-error covariance matrices

The true observation-error covariance matrices $\left(\mathbf{R} = \mathbb{E}\left[\boldsymbol{\epsilon}^{\mathrm{o}}(\boldsymbol{\epsilon}^{\mathrm{o}})^{\top}\right]\right)$ can be estimated directly using samples of $\boldsymbol{\epsilon}^{\mathrm{o}}$ (e.g., Huber, 2004):

$$\begin{aligned}\widehat{\mathbf{R}} &= \frac{1}{N-1}\sum_{i=1}^{N}(\boldsymbol{\epsilon}_i^{\mathrm{o}} - \overline{\boldsymbol{\epsilon}}^{\mathrm{o}})(\boldsymbol{\epsilon}_i^{\mathrm{o}} - \overline{\boldsymbol{\epsilon}}^{\mathrm{o}})^{\top} \\ &= \frac{1}{N-1}\sum_{i=1}^{N}\boldsymbol{\epsilon}_i^{\mathrm{o}}(\boldsymbol{\epsilon}_i^{\mathrm{o}})^{\top} - \overline{\boldsymbol{\epsilon}}^{\mathrm{o}}(\overline{\boldsymbol{\epsilon}}^{\mathrm{o}})^{\top},\end{aligned} \tag{12}$$

where $\widehat{\mathbf{R}}$ denotes the sample observation-error covariance matrix, $\boldsymbol{\epsilon}_i^{\mathrm{o}}$ the ith sample of the observation errors, and $\overline{\boldsymbol{\epsilon}}^{\mathrm{o}} = \frac{1}{N}\sum_{i=1}^{N}\boldsymbol{\epsilon}_i^{\mathrm{o}}$ the sample mean. In this work, any matrix with a hat is a sample estimate of the matrix denoted by the same letter (without a hat). Since the observation error is assumed to be unbiased, the statistical expectation of the sample mean is zero, that is, $\overline{\boldsymbol{\epsilon}}^{\mathrm{o}}$ converges asymptotically to zero as N increases.

4.2 | The Desroziers et al. method

To distinguish it from the direct sampling method given in Section 4.1, we refer to the Desroziers et al. method as the indirect sampling approach in this study. To introduce this method, we first derive an expression for the *innovation covariance matrix* $\mathbf{D} = \mathrm{E}[\mathbf{d}^{\mathrm{b}}(\mathbf{d}^{\mathrm{b}})^{\top}]$. The O−B residual given by Equation (10) is also known as the innovation, which can be rewritten as (Desroziers *et al.*, 2005)

$$\begin{aligned}\mathbf{d}^{\mathrm{b}} &= (\mathbf{y} - H(\mathbf{x}^{\mathrm{t}})) - (H(\mathbf{x}^{\mathrm{b}}) - H(\mathbf{x}^{\mathrm{t}})) \\ &\approx \boldsymbol{\epsilon}^{\mathrm{o}} - \mathbf{H}(\mathbf{x}^{\mathrm{b}} - \mathbf{x}^{\mathrm{t}}) \\ &= \boldsymbol{\epsilon}^{\mathrm{o}} - \mathbf{H}\boldsymbol{\epsilon}^{\mathrm{b}}\end{aligned} \tag{13}$$

using Equations (6) and (7). Then, we obtain

$$\begin{aligned}\mathbf{D} &= \mathbb{E}\left[\boldsymbol{\epsilon}^{\mathrm{o}}(\boldsymbol{\epsilon}^{\mathrm{o}})^{\top}\right] + \mathbf{H}\mathbb{E}\left[\boldsymbol{\epsilon}^{\mathrm{b}}(\boldsymbol{\epsilon}^{\mathrm{b}})^{\top}\right]\mathbf{H}^{\top} \\ &= \mathbf{R} + \mathbf{H}\mathbf{B}\mathbf{H}^{\top},\end{aligned} \tag{14}$$

assuming that $\boldsymbol{\epsilon}^{\mathrm{b}}$ and $\boldsymbol{\epsilon}^{\mathrm{o}}$ are uncorrelated and thus $\mathbb{E}\left[\boldsymbol{\epsilon}^{\mathrm{o}}(\boldsymbol{\epsilon}^{\mathrm{b}})^{\top}\right] = \mathbb{E}\left[\boldsymbol{\epsilon}^{\mathrm{b}}(\boldsymbol{\epsilon}^{\mathrm{o}})^{\top}\right] = \mathbf{0}$. The innovation covariance matrix can also be estimated directly using a finite number of samples using the method of Equation (12) as

$$\widehat{\mathbf{D}} = \frac{1}{N-1}\sum_{i=1}^{N}\mathbf{d}_i^{\mathrm{b}}(\mathbf{d}_i^{\mathrm{b}})^{\top} - \overline{\mathbf{d}}^{\mathrm{b}}(\overline{\mathbf{d}}^{\mathrm{b}})^{\top}, \tag{15}$$

where $\widehat{\mathbf{D}}$ denotes the sample innovation covariance matrix, $\mathbf{d}_i^{\mathrm{b}}$ the ith innovation sample, and $\overline{\mathbf{d}}^{\mathrm{b}} = \frac{1}{N}\sum_{i=1}^{N}\mathbf{d}_i^{\mathrm{b}}$ the sample mean. Since $\mathbb{E}[\boldsymbol{\epsilon}^{\mathrm{o}}]$ and $\mathbb{E}\left[\boldsymbol{\epsilon}^{\mathrm{b}}\right]$ are zero, $\mathbb{E}\left[\mathbf{d}^{\mathrm{b}}\right]$ and $\mathbb{E}\left[\overline{\mathbf{d}}^{\mathrm{b}}\right]$ are zero.

Following the derivation from Desroziers *et al.* (2005), we then substitute Equation (8) into Equation (11) and obtain

$$\mathbf{d}^{\mathrm{a}} = \mathbf{y} - H(\mathbf{x}^{\mathrm{b}} + \widetilde{\mathbf{K}}\mathbf{d}^{\mathrm{b}}), \tag{16}$$

which can be expanded using a Taylor series for a perturbation $\delta\mathbf{x} = \widetilde{\mathbf{K}}\mathbf{d}^{\mathrm{b}}$ about point $\mathbf{x}^{\mathrm{b}}$,

$$\begin{aligned}\mathbf{d}^{\mathrm{a}} &= \mathbf{y} - H(\mathbf{x}^{\mathrm{b}}) - \mathbf{H}\delta\mathbf{x} - \mathcal{O}(\|\delta\mathbf{x}\|^2) \\ &\approx \mathbf{y} - H(\mathbf{x}^{\mathrm{b}}) - \mathbf{H}\widetilde{\mathbf{K}}\mathbf{d}^{\mathrm{b}} \\ &= (\mathbf{I} - \mathbf{H}\widetilde{\mathbf{K}})\mathbf{d}^{\mathrm{b}} \\ &= \widetilde{\mathbf{R}}(\mathbf{H}\widetilde{\mathbf{B}}\mathbf{H}^{\top} + \widetilde{\mathbf{R}})^{-1}\mathbf{d}^{\mathrm{b}}.\end{aligned} \tag{17}$$

Taking the statistical expectation of the outer product of the O−A and O−B residuals gives

$$\begin{aligned}\mathbb{E}\left[\mathbf{d}^{\mathrm{a}}(\mathbf{d}^{\mathrm{b}})^{\top}\right] &= \widetilde{\mathbf{R}}(\mathbf{H}\widetilde{\mathbf{B}}\mathbf{H}^{\top} + \widetilde{\mathbf{R}})^{-1}\mathbb{E}\left[\mathbf{d}^{\mathrm{b}}(\mathbf{d}^{\mathrm{b}})^{\top}\right] \\ &= \widetilde{\mathbf{R}}(\mathbf{H}\widetilde{\mathbf{B}}\mathbf{H}^{\top} + \widetilde{\mathbf{R}})^{-1}(\mathbf{H}\mathbf{B}\mathbf{H}^{\top} + \mathbf{R}) \\ &= \mathbf{R}^{\mathrm{e}},\end{aligned} \tag{18}$$

where $\mathbf{R}^{\mathrm{e}}$ is the *estimated* observation-error covariance matrix (e.g., Janjić *et al.*, 2018; Waller *et al.*, 2016b). When the assumed error covariance matrices ($\widetilde{\mathbf{R}}$ and $\widetilde{\mathbf{B}}$) are equal to the exact covariance matrices $\mathbf{R}$ and $\mathbf{B}$, then $\mathbf{R}^{\mathrm{e}} = \mathbf{R}$. When the assumed matrices do not equal the true matrices, the difference between $\mathbf{R}^{\mathrm{e}}$ and $\mathbf{R}$ is highly dependent on the assumed error statistics. For example, Waller *et al.* (2016b) showed in idealized systems that, when the assumed observation-error covariance matrix $\widetilde{\mathbf{R}}$ is diagonal but the actual errors have spatial correlations, the estimated observation-error standard deviation and correlation length-scale will be smaller than the true statistics.

The matrix $\mathbf{R}^{\mathrm{e}}$ can be estimated by replacing the expected value on the left-hand side of Equation (18) with a sample average (Cordoba *et al.*, 2017; Stewart, 2010, eq. (7.6)),

$$\begin{aligned}\widehat{\mathbf{R}}^{\mathrm{e}} &= \frac{1}{N}\sum_{i=1}^{N}\left(\mathbf{d}_i^{\mathrm{a}} - \overline{\mathbf{d}}^{\mathrm{a}}\right)\left(\mathbf{d}_i^{\mathrm{b}} - \overline{\mathbf{d}}^{\mathrm{b}}\right)^{\top} \\ &= \frac{1}{N}\sum_{i=1}^{N}\mathbf{d}_i^{\mathrm{a}}\left(\mathbf{d}_i^{\mathrm{b}}\right)^{\top} - \overline{\mathbf{d}}^{\mathrm{a}}\left(\overline{\mathbf{d}}^{\mathrm{b}}\right)^{\top},\end{aligned} \tag{19}$$

where $\widehat{\mathbf{R}}^{\mathrm{e}}$ denotes the *indirect* sample observation-error covariance matrix, $\mathbf{d}_i^{\mathrm{a}}$ the ith sample of O−A residuals, and $\overline{\mathbf{d}}^{\mathrm{a}} = \frac{1}{N}\sum_{i=1}^{N}\mathbf{d}_i^{\mathrm{a}}$ the sample mean.

We refer to Equation (19) as the indirect sampling approach used to estimate the observation-error covariance matrix. There are a few things to be aware of when using this equation in practice. First, the standard definition of the Desroziers et al. method (Equation 18) does not guarantee that the estimated observation-error covariance matrix is symmetric. In practice, it may be appropriate to symmetrize the estimated matrix by $\frac{1}{2}\left(\widehat{\mathbf{R}}^{\mathrm{e}} + \left(\widehat{\mathbf{R}}^{\mathrm{e}}\right)^{\top}\right)$. For the purposes of our theoretical analysis, consideration of the symmetrized form would not change any of the results fundamentally, as the Frobenius norm is invariant under matrix transposition. Second, theoretically, the population means of the vectors $\mathbf{d}^{\mathrm{a}}$ and $\mathbf{d}^{\mathrm{b}}$ are zero vectors. However, this may not be the case in practice if, for example, the observations are biased. Regardless of the population means, the sample means of the two vectors are not necessarily zero. Therefore, to obtain unbiased results, the sample means are typically subtracted as done in Equation (19) (Waller *et al.*, 2016a). Third, we follow previous literature and use N as the denominator ((Cordoba *et al.*, 2017; Stewart, 2010, eq. (7.6))). However, it is also possible to use $N-1$ because one degree of freedom is taken to calculate the sample mean $\overline{\mathbf{d}}^{\mathrm{b}}$ (e.g., Field, 2018, p. 106) and the vector $\mathbf{d}^{\mathrm{a}}$ is a function of the vector $\mathbf{d}^{\mathrm{b}}$ (Equation 17). Nevertheless, in practical use of the Desroziers et al. method, the value of N is generally large so that the difference between using N and $N-1$ may be neglected. Fourth, the Desroziers et al. method can be used iteratively in a cycling data assimilation system. Bathmann (2018) has shown that the result of the Desroziers et al. method converges quickly (after a few iterations), and the result of the first iteration does not differ much from the result of the last iteration. Therefore, we do not consider the iteration of the Desroziers et al. method in our analysis. Fifth, the vectors $\mathbf{d}^{\mathrm{a}}$ and $\mathbf{d}^{\mathrm{b}}$ are often assumed to be stationary in time (e.g., a season Waller *et al.*, 2016a, 2016c) or space (e.g., Cordoba *et al.*, 2017). These types of assumption are often made pragmatically using expert opinion, without formal justification, allowing us to use samples taken from different analysis steps or different observation locations to approximate the expected value. Last, the Desroziers et al. diagnostic has been applied successfully in operational systems with nonlinear observation operators (e.g., Michel, 2018; Waller *et al.*, 2019), although the diagnostic derivation assumes that the linear approximation of the observation operator is appropriate. In this study, we address sampling error only in the case of linear observation operators, and further research is needed to determine whether our analysis also holds qualitatively in the case of nonlinear observation operators.

5 | SAMPLING ERROR WITH DIRECT SAMPLING METHOD

In this section, we describe the previous results given by Ledoit and Wolf (2004), where direct sampling error is formulated in terms of key quantities such as the ratio of the number of observations to the number of samples and the average size of the diagonal elements of the matrix. Following Ledoit and Wolf (2004), we measure the size of the sampling error by the *expected quadratic loss* (EQL), defined as

$$\mathrm{EQL}(\widehat{\mathbf{A}}, \mathbf{A}) = \frac{1}{m}\mathbb{E}\left[\|\widehat{\mathbf{A}} - \mathbf{A}\|_{\mathrm{F}}^2\right]. \tag{20}$$

Under three weak assumptions (Assumptions 1-3 of Ledoit & Wolf, 2004), $\mathrm{EQL}(\widehat{\mathbf{A}}, \mathbf{A})$ can be reformulated in terms of four quantities (Appendix A.2 of Ledoit & Wolf, 2004),

$$\frac{1}{m}\mathbb{E}\left[\|\widehat{\mathbf{A}} - \mathbf{A}\|_{\mathrm{F}}^2\right] = \alpha\left[\mu^2(\mathbf{A}) + \theta(\widehat{\mathbf{A}}, \mathbf{A})\right] - \beta(\mathbf{A}). \tag{21}$$

We note that the assumptions used to form Equation (21) are verified for normally or even elliptically distributed random variables, but they are actually much weaker (Ledoit & Wolf, 2004). In addition, Equation (21) holds

only if $\widehat{\mathbf{A}}$ is obtained by sampling directly from $\mathbf{A}$. This means that in our context it can only be used to estimate quantities such as EQL($\widehat{\mathbf{D}}, \mathbf{D}$), but not EQL($\widehat{\mathbf{R}}^{\mathrm{e}}, \mathbf{R}$) or EQL($\widehat{\mathbf{R}}^{\mathrm{e}}, \mathbf{R}^{\mathrm{e}}$).

The first quantity on the right-hand side of Equation (21),

$$\alpha = m/N, \tag{22}$$

is the ratio of the length of the observation-error vector (m) to the sample size (N). We can see from Equation (21) that EQL($\widehat{\mathbf{A}}$, $\mathbf{A}$) increases with α, so, in order to estimate the covariance matrix accurately, the number of samples needs to be much larger than the matrix column dimension (m). The second quantity,

$$\mu^2(\mathbf{A}) = \left[\frac{\mathrm{tr}(\mathbf{A})}{m}\right]^2, \tag{23}$$

is the square of the average size of the diagonal elements of $\mathbf{A}$. For the case of $\mathbf{A} = \mathbf{R}$, the diagonal elements of the true covariance matrix are variances of the observation errors. Therefore, $\mu(\mathbf{R})$ describes the magnitude of the observation error. The quantity $\mu(\mathbf{A})$ can also be given by the average size of the eigenvalues of $\mathbf{A}$, that is, $\mu(\mathbf{A}) = \frac{1}{m}\sum_i^m \lambda_i(\mathbf{A})$ by Equation (5).

To define the third quantity, $\theta(\widehat{\mathbf{A}}, \mathbf{A})$, we first need to introduce another matrix $\mathbf{\Gamma}_{\hat{A},A} \in \mathbb{R}^{m\times N}$, which is obtained by projecting N samples drawn from $\mathbf{A}$ onto the basis given by the eigenvectors of $\mathbf{A}$. In the case of $\mathbf{A} = \mathbf{R}$, we have

$$\mathbf{\Gamma}_{\hat{R},R} = \mathbf{U}_R^{\top}\left[\boldsymbol{\epsilon}_1^{\mathrm{o}}, \boldsymbol{\epsilon}_2^{\mathrm{o}}, \ldots, \boldsymbol{\epsilon}_N^{\mathrm{o}}\right], \tag{24}$$

where $\mathbf{U}_R$ is a matrix containing the eigenvectors of $\mathbf{R}$ and $\boldsymbol{\epsilon}_i^{\mathrm{o}}$ is defined in Section 4.1. The matrix $\mathbf{\Gamma}_{\hat{R},R}$ can be interpreted as a matrix comprising N samples of m uncorrelated observation errors, and it spans the same space as the matrix given by the samples of correlated observation errors, $\boldsymbol{\epsilon}_1^{\mathrm{o}}, \boldsymbol{\epsilon}_2^{\mathrm{o}}, \ldots, \boldsymbol{\epsilon}_N^{\mathrm{o}}$. Using Equation (12) and considering the sample mean to be zero, we may write

$$\frac{1}{N-1}\left[\boldsymbol{\epsilon}_1^{\mathrm{o}}, \boldsymbol{\epsilon}_2^{\mathrm{o}}, \ldots, \boldsymbol{\epsilon}_N^{\mathrm{o}}\right]\left[\boldsymbol{\epsilon}_1^{\mathrm{o}}, \boldsymbol{\epsilon}_2^{\mathrm{o}}, \ldots, \boldsymbol{\epsilon}_N^{\mathrm{o}}\right]^{\top} \approx \mathbf{R}. \tag{25}$$

Then, we have

$$\frac{1}{N-1}\mathbf{\Gamma}_{\hat{R},R}\mathbf{\Gamma}_{\hat{R},R}^{\top} \approx \mathbf{U}_R^{\top}\mathbf{R}\mathbf{U}_R = \mathbf{\Lambda}_R. \tag{26}$$

How close the two quantities on either side of the approximation sign are depends on two things: (1) how well the eigenvectors of the sample covariance matrix match the eigenvectors of the true matrix and (2) how well the eigenvalues of the sample covariance match the eigenvalues of the true matrix. Now, let $\gamma_{i1}(\widehat{\mathbf{A}}, \mathbf{A})$ denote the ith element of the first column of matrix $\mathbf{\Gamma}_{\hat{A},A}$, then the third quantity on the right-hand side of Equation (21) is defined as

$$\theta(\widehat{\mathbf{A}}, \mathbf{A}) = \mathrm{Var}\left[\frac{1}{m}\sum_{i=1}^{m}\gamma_{i1}^2(\widehat{\mathbf{A}}, \mathbf{A})\right], \tag{27}$$

which measures the variance of $m^{-1}\sum_{i=1}^m \gamma_{i1}^2(\widehat{\mathbf{A}}, \mathbf{A})$ in the following equality:

$$\mathbb{E}\left[\left(\frac{1}{m}\sum_{i=1}^{m}\gamma_{i1}^2\right)^2\right] = \left(\mathbb{E}\left[\frac{1}{m}\sum_{i=1}^{m}\gamma_{i1}^2\right]\right)^2 + \mathrm{Var}\left[\frac{1}{m}\sum_{i=1}^{m}\gamma_{i1}^2\right]. \tag{28}$$

In our experiments, the variance is estimated over one thousand realisations of $m^{-1}\sum_{i=1}^m \gamma_{i1}^2(\widehat{\mathbf{A}}, \mathbf{A})$. As noted by Ledoit and Wolf (2004), in general $\theta(\widehat{\mathbf{A}}, \mathbf{A})$ is a non-negligible, positive quantity. However, if the samples are (perfectly) normally distributed, then $\theta(\widehat{\mathbf{A}}, \mathbf{A})$ is zero. The last quantity,

$$\beta(\mathbf{A}) = \frac{1}{mN}\sum_{i=1}^{m}\lambda_i^2(\mathbf{A}), \tag{29}$$

is the sum of the squares of the eigenvalues of $\mathbf{A}$ divided by mN. For any given m, this quantity should be finite, as $\mathbf{A}$ is a finite-dimensional matrix. Thus, it converges to zero as N goes to infinity (Appendix A.2 of Ledoit & Wolf, 2004). However, since we attempt to study sampling error in practical applications where the sample size N is finite, we investigate the variation of $\beta(\mathbf{A})$, as the characteristics of $\mathbf{A}$ change in numerical experiments.

6 | SAMPLING ERROR WITH THE DESROZIERS ET AL. METHOD

In this section, we present our new theoretical results for the sampling error with the Desroziers et al. method, which we refer to as an indirect sampling error. As shown by the following theorem, the indirect sampling error is comprised of three terms.

Theorem 1. *The EQL($\widehat{\mathbf{R}}^{\mathrm{e}}, \mathbf{R}$) can be calculated by*

$$\frac{1}{m}\mathbb{E}\left[\|\widehat{\mathbf{R}}^{\mathrm{e}} - \mathbf{R}\|_{\mathrm{F}}^2\right] = \frac{1}{m}\mathbb{E}\left[\|\widehat{\mathbf{R}}^{\mathrm{e}} - \mathbf{R}^{\mathrm{e}}\|_{\mathrm{F}}^2\right] + \frac{1}{m}\|\mathbf{R}^{\mathrm{e}} - \mathbf{R}\|_{\mathrm{F}}^2 + \frac{2}{m}\left\langle\mathbb{E}\left[\widehat{\mathbf{R}}^{\mathrm{e}} - \mathbf{R}^{\mathrm{e}}\right], \mathbf{R}^{\mathrm{e}} - \mathbf{R}\right\rangle_{\mathrm{F}}. \tag{30}$$

The proof of Theorem 1 is provided in Appendix A. The first term on the right-hand side of Equation (30), which can be denoted by EQL($\widehat{\mathbf{R}}^{\mathrm{e}}, \mathbf{R}^{\mathrm{e}}$), measures an indirect sampling error, where the matrix $\mathbf{R}^{\mathrm{e}}$ is calculated by Equation (18) and matrix $\widehat{\mathbf{R}}^{\mathrm{e}}$ is calculated by Equation (19). We remind the reader that $\mathbf{R}^{\mathrm{e}}$ and $\widehat{\mathbf{R}}^{\mathrm{e}}$ are both estimates from the Desroziers et al. method, but $\mathbf{R}^{\mathrm{e}}$ is a theoretical estimate in exact arithmetic (no sampling error) and $\widehat{\mathbf{R}}^{\mathrm{e}}$ is calculated from samples of O−A and O−B residuals. We note that EQL($\widehat{\mathbf{R}}^{\mathrm{e}}, \mathbf{R}^{\mathrm{e}}$) does not measure direct sampling errors because $\widehat{\mathbf{R}}^{\mathrm{e}}$ is not obtained using the samples that are directly drawn from $\mathbf{R}^{\mathrm{e}}$. How to estimate this term can be found below in Theorem 3. The second term on the right-hand side of Equation (30), $\frac{1}{m}\|\mathbf{R}^{\mathrm{e}} - \mathbf{R}\|_{\mathrm{F}}^2$, measures the difference between the estimated and true observation-error covariance matrices, which is determined by the accuracy of the assumed background and observation-error statistics and is invariant to sample size. These errors were investigated by Waller *et al.* (2016b). Experiments with real data (e.g., Waller *et al.*, 2016c) have shown qualitatively similar results. The last term, $\frac{2}{m}\left\langle \mathbb{E}\left[\widehat{\mathbf{R}}^{\mathrm{e}} - \mathbf{R}^{\mathrm{e}}\right], \mathbf{R}^{\mathrm{e}} - \mathbf{R}\right\rangle_{\mathrm{F}}$, is expected to be zero because $\mathbb{E}\left[\widehat{\mathbf{R}}^{\mathrm{e}}\right] = \mathbf{R}^{\mathrm{e}}$. In practice, however, this term may not be negligible, since $\widehat{\mathbf{R}}^{\mathrm{e}}$ is estimated using a finite sample size.

We note that, in a special case where the assumed background and observation-error covariances are exactly the same as the true background and observation-error covariances, respectively (i.e., $\widetilde{\mathbf{B}} = \mathbf{B}$ and $\widetilde{\mathbf{R}} = \mathbf{R}$), we have $\mathbf{R}^{\mathrm{e}} = \mathbf{R}$ and thus the second and third terms on the right-hand side of Equation (30) vanish.

Since the third term on the right-hand side of Equation (30) may be expensive to calculate in practical applications, we further provide an upper bound on EQL($\widehat{\mathbf{R}}^{\mathrm{e}}, \mathbf{R}$) that is determined only by the first two terms on the right-hand side of Equation (30).

Theorem 2. *The EQL($\widehat{\mathbf{R}}^{\mathrm{e}}, \mathbf{R}$) can be bounded by the following inequality*

$$\frac{1}{m}\mathbb{E}\left[\|\widehat{\mathbf{R}}^{\mathrm{e}} - \mathbf{R}\|_{\mathrm{F}}^2\right] \leqslant \frac{1}{m}\mathbb{E}\left[\|\widehat{\mathbf{R}}^{\mathrm{e}} - \mathbf{R}^{\mathrm{e}}\|_{\mathrm{F}}^2\right] + \frac{1}{m}\|\mathbf{R}^{\mathrm{e}} - \mathbf{R}\|_{\mathrm{F}}^2 + 2\sqrt{\frac{1}{m}\mathbb{E}\left[\|\widehat{\mathbf{R}}^{\mathrm{e}} - \mathbf{R}^{\mathrm{e}}\|_{\mathrm{F}}^2\right] \cdot \frac{1}{m}\|\mathbf{R}^{\mathrm{e}} - \mathbf{R}\|_{\mathrm{F}}^2}. \quad (31)$$

The proof of Theorem 2 is given in Appendix B. We now provide a theorem that can be used to estimate the size of $\frac{1}{m}\mathbb{E}\left[\|\widehat{\mathbf{R}}^{\mathrm{e}} - \mathbf{R}^{\mathrm{e}}\|_{\mathrm{F}}^2\right]$. As shown by Equation (17), the O−A residual vector, $\mathbf{d}^{\mathrm{a}}$, is a function of the O−B innovation vector, $\mathbf{d}^{\mathrm{b}}$. Thus, we may write

$$\mathbf{R}^{\mathrm{e}} = \widetilde{\mathbf{W}}\mathbf{D} \quad (32)$$

and

$$\widehat{\mathbf{R}}^{\mathrm{e}} = \widetilde{\mathbf{W}}\widehat{\mathbf{D}}, \quad (33)$$

where $\widetilde{\mathbf{W}} = \widetilde{\mathbf{R}}(\mathbf{H}\widetilde{\mathbf{B}}\mathbf{H}^{\mathrm{T}} + \widetilde{\mathbf{R}})^{-1}$ is an $m \times m$ matrix, which is not necessarily symmetric, and the true innovation covariance matrix, $\mathbf{D}$, and its sample matrix, $\widehat{\mathbf{D}}$, are defined by Equations (14) and (15), respectively. Using Equations (32) and (33), we obtain the following theorem:

Theorem 3. *The EQL($\widehat{\mathbf{R}}^{\mathrm{e}}, \mathbf{R}^{\mathrm{e}}$) can be bounded by the following inequality*

$$\frac{1}{m}\mathbb{E}\left[\|\widehat{\mathbf{R}}^{\mathrm{e}} - \mathbf{R}^{\mathrm{e}}\|_{\mathrm{F}}^2\right] = \frac{1}{m}\mathbb{E}\left[\|\widetilde{\mathbf{W}}(\widehat{\mathbf{D}} - \mathbf{D})\|_{\mathrm{F}}^2\right] \leqslant s_1^2(\widetilde{\mathbf{W}}) \cdot \frac{1}{m}\mathbb{E}\left[\|\widehat{\mathbf{D}} - \mathbf{D}\|_{\mathrm{F}}^2\right], \quad (34)$$

where $s_1^2(\widetilde{\mathbf{W}})$ is the square of the largest singular value of $\widetilde{\mathbf{W}}$.

More details on singular-value decomposition (SVD) and the properties of singular values can be found in Bernstein (2009, chapter 5). The proof of the upper bound shown in Theorem 3 is shown in Appendix C. The term $\frac{1}{m}\mathbb{E}\left[\|\widehat{\mathbf{D}} - \mathbf{D}\|_{\mathrm{F}}^2\right]$ in Equation (34) is a measure of direct sampling errors, which can be calculated using Equation (21). In practical applications, we cannot calculate $\frac{1}{m}\mathbb{E}\left[\|\widehat{\mathbf{D}} - \mathbf{D}\|_{\mathrm{F}}^2\right]$ exactly, as the true innovation covariance matrix ($\mathbf{D}$) is unknown, but we know that this term decreases as the sample size increases, regardless of the structure of the matrix $\mathbf{D}$. The term, $s_1^2(\widetilde{\mathbf{W}})$, has an upper bound given by the following inequality:

$$s_1^2(\widetilde{\mathbf{W}}) \leqslant \left(\frac{\lambda_1(\widetilde{\mathbf{R}})}{\lambda_m(\widetilde{\mathbf{R}}) + \lambda_m(\mathbf{H}\widetilde{\mathbf{B}}\mathbf{H}^{\mathrm{T}})}\right)^2. \quad (35)$$

For a proof of this inequality see Appendix D. In addition to Equation (35), if the matrices $\widetilde{\mathbf{R}}$, $\mathbf{H}\widetilde{\mathbf{B}}\mathbf{H}^{\mathrm{T}}$, and $\widetilde{\mathbf{W}}$ are circulant, then the size of $s_1^2(\widetilde{\mathbf{W}})$ can be calculated easily without forming the matrix $\widetilde{\mathbf{W}}$. (The definition of circulant matrices and their properties as well as the calculation of $s_1^2(\widetilde{\mathbf{W}})$ are provided in Appendix E.) More generally, for many observation types assimilated operationally, the observation-error covariance matrix ($\widetilde{\mathbf{R}}$) is assumed diagonal and its eigenvalues are simply the diagonal elements of this matrix. For observation types where the matrix $\widetilde{\mathbf{R}}$ has a more complex structure, these matrices are usually relatively small (e.g., satellite interchannel error covariances of order 100 × 100) and so the eigenvalues can be calculated directly. The term $\lambda_m(\mathbf{H}\widetilde{\mathbf{B}}\mathbf{H}^{\mathrm{T}})$ depends on the background-error covariance, which is not typically available in explicit form in variational assimilation. However, it can be approximated using a "randomisation" method

(Anderson *et al.*, 2000; Tabeart *et al.*, 2020a) in order to provide an estimate of the bound in Equation (35).

Corollary 1. *Theorem 3 can also be applied to a particular case where the assumed error statistics are exact (i.e.,* $\widetilde{\mathbf{B}} = \mathbf{B}$ *and* $\widetilde{\mathbf{R}} = \mathbf{R}$*). In this case, we have* $\widetilde{\mathbf{W}} = \mathbf{W}$ *and* $\mathbf{R}^{\mathrm{e}} = \mathbf{R}$*, which gives*

$$\frac{1}{m}\mathbb{E}\left[\|\widehat{\mathbf{R}}^{\mathrm{e}} - \mathbf{R}\|_{\mathrm{F}}^2\right] = \frac{1}{m}\mathbb{E}\left[\|\mathbf{W}(\widehat{\mathbf{D}} - \mathbf{D})\|_{\mathrm{F}}^2\right] \leqslant s_1^2(\mathbf{W}) \cdot \frac{1}{m}\mathbb{E}\left[\|\widehat{\mathbf{D}} - \mathbf{D}\|_{\mathrm{F}}^2\right]. \quad (36)$$

We will use simple numerical experiments to illustrate these theoretical analyses of the sampling error with the Desroziers et al. method (Section 8).

7 | EIGENVALUES OF THE ESTIMATED OBSERVATION-ERROR COVARIANCE MATRICES

Several studies have shown that the eigenspectrum of the estimated observation-error covariance matrix influences the numerical convergence of variational assimilation schemes (e.g., Campbell *et al.*, 2017; Tabeart *et al.*, 2018, 2020a, 2021; Weston *et al.*, 2014). We therefore investigate how the sampling error affects the eigenvalues of the estimated matrices in this section. Let

$$\delta(\mathbf{A}) = \frac{1}{m}\sum_{i=1}^{m}(\lambda_i(\mathbf{A}) - \mu(\mathbf{A}))^2 \quad (37)$$

denote the spread of the eigenvalues of $\mathbf{A}$, where $\mu(\mathbf{A}) = \frac{1}{m}\sum_i^m \lambda_i(\mathbf{A})$ is the same quantity defined by the trace in Equation (23). Following Ledoit and Wolf (2004), we then define

$$\mathbb{E}\left[\delta(\widehat{\mathbf{A}})\right] = \frac{1}{m}\mathbb{E}\left[\sum_{i=1}^{m}(\lambda_i(\widehat{\mathbf{A}}) - \mu(\mathbf{A}))^2\right] \quad (38)$$

as the *cross-sectional dispersion of sample eigenvalues*, which describes the spread of the eigenvalues of $\widehat{\mathbf{A}}$ around the mean of the eigenvalues of $\mathbf{A}$. Ledoit and Wolf (2004, eq. (12)) showed that the cross-sectional dispersion of sample eigenvalues is equal to the sum of $\delta(\mathbf{A})$ and $\mathrm{EQL}(\widehat{\mathbf{A}}, \mathbf{A})$ under the assumption that $\mathbb{E}\left[\widehat{\mathbf{A}}\right] = \mathbf{A}$, that is,

$$\mathbb{E}\left[\delta(\widehat{\mathbf{A}})\right] = \delta(\mathbf{A}) + \frac{1}{m}\mathbb{E}\left[\|\widehat{\mathbf{A}} - \mathbf{A}\|_{\mathrm{F}}^2\right]. \quad (39)$$

Since the expected quadratic loss, $\frac{1}{m}\mathbb{E}\left[\|\widehat{\mathbf{A}} - \mathbf{A}\|_{\mathrm{F}}^2\right]$, is positive, Equation (39) indicates that the eigenvalues of $\widehat{\mathbf{A}}$ are expected to be more dispersed around $\mu(\mathbf{A})$ than the eigenvalues of $\mathbf{A}$, and the excess dispersion is given by the sampling error of $\widehat{\mathbf{A}}$. In the case of direct sampling, we have

$$\mathbb{E}\left[\delta(\widehat{\mathbf{R}})\right] = \delta(\mathbf{R}) + \frac{1}{m}\mathbb{E}\left[\|\widehat{\mathbf{R}} - \mathbf{R}\|_{\mathrm{F}}^2\right] \quad (40)$$

and the excess dispersion implies that the largest sample eigenvalues are bigger than the corresponding true eigenvalues, while the smallest sample eigenvalues are less than the corresponding true eigenvalues (for an illustration see Figure 10). In the case of indirect sampling with exact assumed error statistics, we still have

$$\mathbb{E}\left[\delta(\widehat{\mathbf{R}}^{\mathrm{e}})\right] = \delta(\mathbf{R}) + \frac{1}{m}\mathbb{E}\left[\|\widehat{\mathbf{R}}^{\mathrm{e}} - \mathbf{R}\|_{\mathrm{F}}^2\right]. \quad (41)$$

In the above two cases, the cross-sectional dispersion of the eigenvalues of the estimated observation-error covariance matrices is always larger than the spread of the true eigenvalues, and their difference increases as the sampling error increases. This is undesirable, as the larger dispersion will result in a higher condition number of the matrix and a larger condition number will slow down the convergence of the variational minimisation (e.g., Campbell *et al.*, 2017; Tabeart *et al.*, 2018, 2020a, 2021; Weston *et al.*, 2014).

In the case of indirect sampling with inexact assumed error statistics, $\mathbb{E}\left[\widehat{\mathbf{R}}^{\mathrm{e}}\right]$ is equal to $\mathbf{R}^{\mathrm{e}}$ rather than $\mathbf{R}$. Therefore, we need to derive a more general expression than Equation (39), where the assumption of $\mathbb{E}\left[\widehat{\mathbf{A}}\right] = \mathbf{A}$ is not needed.

Theorem 4. *In general, the cross-sectional dispersion of sample eigenvalues is given by*

$$\mathbb{E}\left[\delta(\widehat{\mathbf{A}})\right] = \delta(\mathbf{A}) + \frac{2}{m}\left\langle\mathbb{E}\left[\widehat{\mathbf{A}} - \mathbf{A}\right], \mathbf{A} - \mu(\mathbf{A})\cdot\mathbf{I}\right\rangle_{\mathrm{F}} + \frac{1}{m}\mathbb{E}\left[\|\widehat{\mathbf{A}} - \mathbf{A}\|_{\mathrm{F}}^2\right], \quad (42)$$

where $\delta(\mathbf{A})$ *and* $\mathbb{E}\left[\delta(\widehat{\mathbf{A}})\right]$ *are defined by Equations (37) and (38), respectively.*

The proof of Theorem 4 can be found in Appendix F. Comparing Equations (39) and (42), we see that Equation (42) has an extra Frobenius inner-product term given by $\frac{2}{m}\left\langle\mathbb{E}\left[\widehat{\mathbf{A}} - \mathbf{A}\right], \mathbf{A} - \mu(\mathbf{A})\cdot\mathbf{I}\right\rangle_{\mathrm{F}}$. In the particular case where $\mathbb{E}\left[\widehat{\mathbf{A}}\right] = \mathbf{A}$, the Frobenius inner-product term is zero and Equations (39) and (42) are equivalent. More generally, this term could be positive or negative, and, depending on its value, could lead to underdispersion or excess dispersion of the eigenvalues (as will be seen in our numerical results shown by Figure 9). In our case, we

have the following corollary of Theorem 4:

$$\mathbb{E}\left[\delta(\widehat{\mathbf{R}}^{\mathrm{e}})\right] = \delta(\mathbf{R}) + \frac{2}{m}\langle \mathbb{E}\left[\widehat{\mathbf{R}}^{\mathrm{e}} - \mathbf{R}\right], \mathbf{R} - \mu(\mathbf{R})\cdot\mathbf{I}\rangle_{\mathrm{F}} + \frac{1}{m}\mathbb{E}\left[\|\widehat{\mathbf{R}}^{\mathrm{e}} - \mathbf{R}\|_{\mathrm{F}}^2\right]. \tag{43}$$

In Section 8.5, we examine the cross-sectional dispersion of eigenvalues in cases of direct and indirect sampling using simple numerical experiments. We also investigate the difference between the eigenvalue spectra of the sample and true observation-error covariance matrices.

8 | NUMERICAL EXPERIMENTS

We now carry out some numerical experiments. These experiments cannot cover every situation that arises in practice. For example, our assumed background-error covariance matrices are always identical to the true ones (see Equation (50)). The purpose of these experiments is twofold: firstly, to illustrate some of the key features of the theoretical analysis; secondly, to present some examples of the potential use of the theoretical results in practical applications. Since we focus on the sampling error in the estimation of observation-error covariance matrices, it is not necessary to conduct a complete data assimilation experiment. Our experimental design is described in Section 8.1. We note that in our experiments the matrices $\mathbf{R}$, $\widetilde{\mathbf{R}}$, $\mathbf{HBH}^{\mathrm{T}}$, and $\mathbf{H}\widetilde{\mathbf{B}}\mathbf{H}^{\mathrm{T}}$ are circulant by the way we construct them and thus our interpretation of the experimental results is based on the properties of circulant matrices (for details on circulant matrices see e.g., Gray, 2006). However, the theorems presented in Sections 6 and 7 do not require the matrices to be circulant.

8.1 | Experimental design

We assume our $n = 2000$ model state grid points (where $\mathbf{x}^{\mathrm{t}}$, $\mathbf{x}^{\mathrm{b}}$, and $\mathbf{x}^{\mathrm{a}}$ are located) to be equally spaced on a circle with radius 6371 km (e.g., Tabeart *et al.*, 2018) and our $m = 1000$ observations ($\mathbf{y}$) to be taken at alternate grid points. This leads to the observation operator H becoming an $m \times n$ matrix containing only zeroes and ones, where $n = 2m$, that is,

$$\mathbf{H}_{i,j} = \begin{cases} 1, & \text{if } j = 2i-1 \text{ for } i = 1, \ldots, m, \\ 0, & \text{otherwise.} \end{cases} \tag{44}$$

In this case, $\mathbf{HBH}^{\mathrm{T}}$ is the matrix formed by deleting every second row and column of the matrix $\mathbf{B}$.

The observation errors are taken from a multivariate Gaussian distribution with zero mean and covariance $\mathbf{R}$,

$$\boldsymbol{\epsilon}_i^{\mathrm{o}} \sim \mathcal{N}(0, \mathbf{R}), \quad \text{for } i = 1, \ldots, N. \tag{45}$$

Similarly, the samples of the O−B residual defined by Equation (10) are drawn from a multivariate Gaussian distribution with zero mean and covariance $\mathbf{R} + \mathbf{HBH}^{\mathrm{T}}$,

$$\mathbf{d}_i^{\mathrm{b}} \sim \mathcal{N}(0, \mathbf{R} + \mathbf{HBH}^{\mathrm{T}}) \quad \text{for } i = 1, \ldots, N. \tag{46}$$

We used the Python function *numpy.random.multivariate_normal* to generate $\boldsymbol{\epsilon}_i^{\mathrm{o}}$ and $\mathbf{d}_i^{\mathrm{b}}$ (Harris *et al.*, 2020). This function produces pseudo-random numbers using the Mersenne Twister method (e.g., Haramoto *et al.*, 2008) and uses a SVD to factorise the covariance matrix. Finally, the samples of the O−A residual defined by Equation (11) are calculated from the samples of the O−B residual using Equation (17) to give

$$\mathbf{d}_i^{\mathrm{a}} = \widetilde{\mathbf{R}}(\mathbf{H}\widetilde{\mathbf{B}}\mathbf{H}^{\mathrm{T}} + \widetilde{\mathbf{R}})^{-1}\mathbf{d}_i^{\mathrm{b}}, \quad \text{for } i = 1, \ldots, N. \tag{47}$$

We generate true observation-error covariance matrices using the first-order auto-regressive (FOAR) correlation function, which is used in practical applications to model Doppler radar wind observation-error statistics (Simonin *et al.*, 2019). The formula is

$$\mathbf{R}(i,j) = \sigma_{\mathrm{o}}^2 \exp\left(\frac{-|\Delta_{i,j}^{y}|}{l_{\mathrm{o}}}\right), \tag{48}$$

where σ_{o} denotes the observation-error standard deviation, $\Delta_{i,j}^{y}$ denotes the distance between the ith and jth observations, and l_{o} denotes the observation-error correlation length-scale. The distance between two observations is calculated using chordal distance rather than great-circle distance, as the former ensures that the resulting covariance matrix is positive-definite (Haben, 2011, p. 52; Jeong & Jun, 2015; Tabeart, 2019, p. 34; Yaglom, 1987). Since, in operational NWP data assimilation, correlated observation errors are sometimes assumed to be uncorrelated, we create the assumed observation-error covariance matrix as a diagonal matrix with diagonal elements that are the assumed observation-error variance $\widetilde{\sigma}_{\mathrm{o}}^2$:

$$\widetilde{\mathbf{R}} = \widetilde{\sigma}_{\mathrm{o}}^2\mathbf{I}. \tag{49}$$

The true and assumed background-error covariance matrices are formed using the second-order auto-regressive (SOAR) correlation function, which is sometimes used to model background-error covariance matrices in

practical applications (e.g., Ballard *et al.*, 2016). The equation is

$$\mathbf{B}(i,j) = \widetilde{\mathbf{B}}(i,j) = \sigma_{\mathrm{b}}^2\left(1 + \frac{|\Delta_{i,j}^x|}{l_{\mathrm{b}}}\right)\exp\left(\frac{-|\Delta_{i,j}^x|}{l_{\mathrm{b}}}\right), \quad (50)$$

where σ_{b} denotes the background-error standard deviation, l_{b} denotes the background-error correlation length-scale, and $\Delta_{i,j}^x$ denotes the chordal distance between the ith and jth model state grid points.

In our experiments, the values of σ_{o}, $\widetilde{\sigma}_{\mathrm{o}}$, and σ_{b} vary from 0.4–1.6 with an interval of 0.2, and the values of l_{o} and l_{b} range from 20–140 km with 20-km intervals. These values are selected by considering those estimated for real geostationary satellite observations (Waller *et al.*, 2016a) or used in an operational km-scale NWP system (Ballard *et al.*, 2016). When $l_{\mathrm{o}} = 20$ km, the observation-error covariance matrix obtained is close to the diagonal matrix; the off-diagonal elements drop to almost zero at an offset of 2 from the main diagonal. The specific parameter values used for each experiment are listed in Table 1. The result of each experiment is averaged over 1000 realisations of that experiment. It should also be noted that, in our experiments, the matrix $\widehat{\mathbf{R}}^{\mathrm{e}}$ is symmetrized by taking the average of itself and its transpose (see discussion in the last paragraph of Section 4.2).

8.2 | Direct sampling error experiments

The direct sampling approach (Equation 12) cannot be applied in practical applications, as the true observation-error covariance matrix ($\mathbf{R}$) is unknown. Thus, the numerical results for direct sampling shown in this section are for illustrative purposes only. They may assist the reader in understanding the later results on indirect sampling error better. In the following experiments, we show how the expected quadratic loss of the sample observation-error covariance matrix ($\widehat{\mathbf{R}}$), EQL($\widehat{\mathbf{R}}, \mathbf{R}$), varies with the true observation-error standard deviation (σ_{o}) and correlation length-scale (l_{o}). As discussed in Section 5, the size of EQL($\widehat{\mathbf{R}}, \mathbf{R}$) is determined by four quantities: (1) the ratio of the number of observations (m) to sample size (N), $\alpha = m/N$; (2) the square of the average size of the diagonal elements of the matrix $\mathbf{R}$, $\mu^2(\mathbf{R})$; (3) a variance term, $\theta(\widehat{\mathbf{R}}, \mathbf{R})$ (see Equation 27 for more information); and (4) the sum of the squares of the eigenvalues of the matrix $\mathbf{R}$ divided by mN, $\beta(\mathbf{R})$. We also show how the last three quantities vary with the true observation-error standard deviation and correlation length-scale for different values of the ratio α.

8.2.1 | Varying observation-error standard deviation

Figure 1 shows direct sampling error, EQL($\widehat{\mathbf{R}}, \mathbf{R}$) (Equation 20), and three quantities $\mu^2(\mathbf{R})$, $\theta(\widehat{\mathbf{R}}, \mathbf{R})$, and $\beta(\mathbf{R})$ (Equations 23–29) as a function of observation-error standard deviation (σ_{o}). Each panel uses a different ratio (α) of the number of observations (m) to sample size (N). EQL($\widehat{\mathbf{R}}, \mathbf{R}$) is calculated as a standalone term by Equation (20) rather than from the quantities on the right-hand side of Equation (21). These two

TABLE 1 The values of the ratio of the number of observations to sample size (α), observation-error standard deviation (σ_{o}), assumed observation-error standard deviation ($\widetilde{\sigma}_{\mathrm{o}}$), background-error standard deviation (σ_{b}), observation-error correlation length-scale (l_{o}), and background-error correlation length-scale (l_{b}) used in each figure in Section 8.

	α	σ_{o}	σ_{b}	l_{o}	l_{b}	$\widetilde{\sigma}_{\mathrm{o}}$
Figure 1	0.1, 1, 10	0.4, 0.6, … , 1.6	—	80	—	—
Figure 2	0.1, 1, 10	1.0	—	20, 40, … , 140	—	—
Figure 3	0.1, 1, 10	0.4, 0.6, … , 1.6	0.6	80	20	—
Figure 4	0.1, 1, 10	1.0	0.4, 0.6, … , 1.6	80	20	—
Figure 5	0.1	1.0	0.6	20, 40, … , 140	20, 40, … , 140	—
Figure 6	0.1	1.0	0.6	80	20	0.4, 0.6, … , 1.6
Figure 7	0.1	1.0	0.6	20, 40, … , 140	20	1.0
Figure 8	0.01, 0.02, 0.05, 0.1, 0.2, 0.5, 1.0, 2, 5, 10	1.0	0.6	80	20	1.0
Figure 9	0.01, 0.02, 0.05, 0.1, 0.2, 0.5, 1.0, 2, 5, 10	1.0	0.6	80	20	1.0, 4.0
Figure 10	0.1	1.0	0.6	80	20	—
Figure 11	0.1	1.0	0.6	80	20	0.4, 1.0, 4.0

Note: The number of observations is $m = 1000$ for all figures. For Figures 6–9 and 11, the assumed observation-error covariance matrix is diagonal, that is, $\widetilde{\mathbf{R}} = \widetilde{\sigma}_{\mathrm{o}}^2\mathbf{I}$, and the assumed and true background-error covariance matrices are identical, that is, $\widetilde{\mathbf{B}} = \mathbf{B}$.

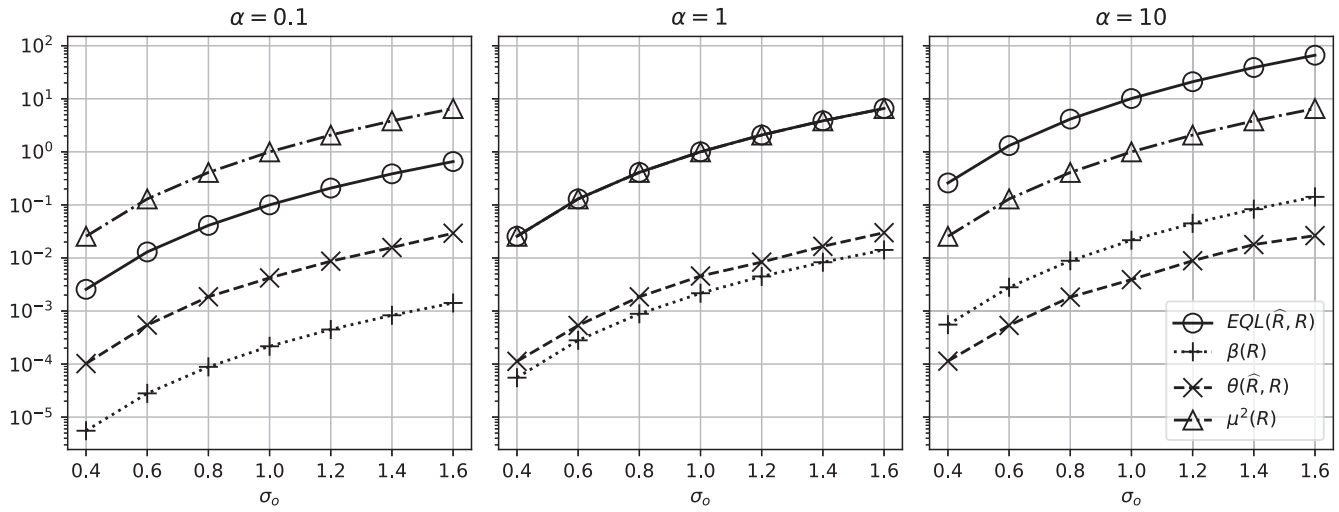

FIGURE 1 Direct sampling error given by EQL($\widehat{\mathbf{R}}, \mathbf{R}$) and the quantities $\mu^2(\mathbf{R})$, $\theta(\widehat{\mathbf{R}}, \mathbf{R})$, and $\beta(\mathbf{R})$ (Equation 21) as a function of observation-error standard deviation (σ_o) for three different ratios (α) of the number of observations to sample size. The y-axis is plotted using a log scale.

equations do not give the same value, due to the sampling error in the estimation of $\theta(\widehat{\mathbf{R}}, \mathbf{R})$. In our experiments, the values of $\theta(\widehat{\mathbf{R}}, \mathbf{R})$ and $\frac{1}{m}\mathbb{E}\left[\|\widehat{\mathbf{R}} - \mathbf{R}\|_F^2\right]$ are estimated using 1000 realisations of $\widehat{\mathbf{R}}$ calculated using Equation (12), and the uncertainty in the estimation is negligible.

By comparing the three panels of Figure 1, we find that the direct sampling errors increase as the ratio $\alpha = m/N$ increases. This result is clearly indicated by Equation (21). By looking at each panel, we find that the square of the average size of the diagonal elements of the matrix $\mathbf{R}$, $\mu^2(\mathbf{R})$, increases as σ_o increases. An explanation for this is given by the following equations. If we assume that the true observation-error covariance matrix is modelled by

$$\mathbf{R} = \sigma_o^2 \mathbf{C}, \tag{51}$$

where $\mathbf{C} \in \mathbb{R}^{m \times m}$ is an arbitrary correlation matrix, then using Equation (23) we obtain

$$\mu^2(\mathbf{R}) = \sigma_o^4, \tag{52}$$

which explains the increase of $\mu^2(\mathbf{R})$ with σ_o. Moreover, as $\mu^2(\mathbf{R})$ is not affected by α, the curve with triangles is the same in each panel in Figure 1.

The quantity $\beta(\mathbf{R})$ is also found to increase with σ_o, which can be explained by substituting Equation (51) into Equation (29),

$$\beta(\mathbf{R}) = \frac{\sigma_o^4}{mN} \sum_{i=1}^{m} \lambda_i^2(\mathbf{C}). \tag{53}$$

Equation (53) also explains why an increase in $\alpha = m/N$ results in an increase in $\beta(\mathbf{R})$ as shown in Figure 1. (Note that, from the left to the right panel, the sample size, N, decreases while the number of observations, m, remains the same.) Comparing Equations (52) and (53), we can see that $\beta(\mathbf{R})$ should be a smaller quantity than $\mu^2(\mathbf{R})$, as shown by Figure 1.

The variance term, $\theta(\widehat{\mathbf{R}}, \mathbf{R})$, also varies with σ_o. This term is calculated using the matrix $\mathbf{\Gamma}_{\widehat{R},R}$, the columns of which are samples of uncorrelated normal random variables with standard deviation σ_o. Figure 1 shows that, like the other quantities, $\theta(\widehat{\mathbf{R}}, \mathbf{R})$ increases as σ_o increases (see the curve with crosses in Figure 1). This is because, by substituting Equation (51) into Equation (27), we may write

$$\theta(\widehat{\mathbf{R}}, \mathbf{R}) = \sigma_o^4 \mathrm{Var}\left[\frac{1}{m}\sum_{i=1}^{m} \gamma_{i1}^2(\widehat{\mathbf{C}}, \mathbf{C})\right]. \tag{54}$$

In Figure 1, the quantity $\theta(\widehat{\mathbf{R}}, \mathbf{R})$ is found to be much smaller than $\mu^2(\mathbf{R})$. In addition, $\theta(\widehat{\mathbf{R}}, \mathbf{R})$ is found to be larger than $\beta(\mathbf{R})$ for $\alpha = 0.1$ and 1.0, but smaller than $\beta(\mathbf{R})$ for $\alpha = 10$. This is because an increase in α (meaning a decrease in sample size in our experiment) leads to an increase in $\beta(\mathbf{R})$, but almost no change in $\theta(\widehat{\mathbf{R}}, \mathbf{R})$. (Small changes in $\theta(\widehat{\mathbf{R}}, \mathbf{R})$ may occur, as it is a sample estimate.)

Using Equations (21) and (52)–(54), we may write

$$\mathrm{EQL}(\widehat{\mathbf{R}}, \mathbf{R}) = \sigma_o^4 \left\{ \frac{2}{mN} \sum_{i<j}^{m} \lambda_i(\mathbf{C})\lambda_j(\mathbf{C}) + \frac{m}{N} \cdot \mathrm{Var}\left[\frac{1}{m}\sum_{i=1}^{m} \gamma_{i1}^2(\widehat{\mathbf{C}}, \mathbf{C})\right] \right\}, \tag{55}$$

which shows that, for a given m and a given N, the size of the direct sampling error, EQL($\widehat{\mathbf{R}}, \mathbf{R}$), is proportional to the fourth power of the observation-error standard

deviation (σ_o). This is consistent with the results shown in Figure 1. The derivation of Equation (55) holds if the observation-error covariance matrix can be written in the form of Equation (51) and does not require any particular choice of the correlation matrix $\mathbf{C}$. We will show in the following section that the observation-error correlation length-scale (l_o) has a much smaller impact on the size of EQL($\hat{\mathbf{R}}, \mathbf{R}$) compared with σ_o.

8.2.2 | Varying observation-error correlation length-scale

In this section, we conduct numerical experiments on direct sampling error using different observation-error correlation length-scales (l_o). By definition, the quantity $\mu^2(\mathbf{R})$ depends only on the diagonal elements of $\mathbf{R}$. Therefore, a change in l_o does not affect $\mu^2(\mathbf{R})$, since it does not change the diagonal elements. This is clearly shown by the curve with triangles in Figure 2. How $\beta(\mathbf{R})$ (the sum of the squares of the eigenvalues of the matrix $\mathbf{R}$ divided by mN) varies with l_o depends on the correlation function we use to create the observation-error covariance matrices, as they have different eigenvalue spectra. How the variance term, $\theta(\hat{\mathbf{R}}, \mathbf{R})$, varies with l_o is also not obvious from Equation (54). In our experiments, we find that both $\beta(\mathbf{R})$ and $\theta(\hat{\mathbf{R}}, \mathbf{R})$ increase with l_o as shown by the curves with plus and cross in Figure 2, respectively. We also find that the direct sampling error, EQL($\hat{\mathbf{R}}, \mathbf{R}$), remains almost unchanged with varying l_o in each panel. This is because $\beta(\mathbf{R})$ and $\theta(\hat{\mathbf{R}}, \mathbf{R})$ are much smaller quantities than $\mu^2(\mathbf{R})$ and their influence on the size of EQL($\hat{\mathbf{R}}, \mathbf{R}$) is tiny.

8.3 | Experiments on sampling error with the Desroziers et al. method (exact assumed error statistics)

In this section, we show experimental results on the indirect sampling error with the Desroziers et al. method in the case where the observation and background-error covariance matrices describe the true error statistics completely correctly. This is not what actually happens in practice, but we show the results in this particular case because they will be used later in a more general case. In these experiments, we show the change in the sampling error with the Desroziers et al. method using exact assumed error statistics and its upper bound given by Corollary 1, as the observation and background-error standard deviations and correlation length-scales vary.

8.3.1 | Varying observation and background-error standard deviations

Figure 3 shows that the sampling error with the Desroziers et al. method using exact assumed error statistics (EQL($\hat{\mathbf{R}}^e, \mathbf{R}$)) increases as the observation-error standard deviation (σ_o) increases. In this experiment, the variation of EQL($\hat{\mathbf{R}}^e, \mathbf{R}$) follows closely from the variation of its bound, given by the product of direct sampling error in the estimate of the innovation covariance, EQL($\hat{\mathbf{D}}, \mathbf{D}$), and $s_1^2(\mathbf{W})$ (Corollary 1). (The reader is reminded that $s_1^2(\mathbf{W})$ is the square of the largest singular value of the matrix $\mathbf{W} = \mathbf{R}(\mathbf{HBH}^T + \mathbf{R})^{-1}$.) In general, how tight this bound is depends on two things. Following the derivation of this bound given in Appendix C, the difference between the

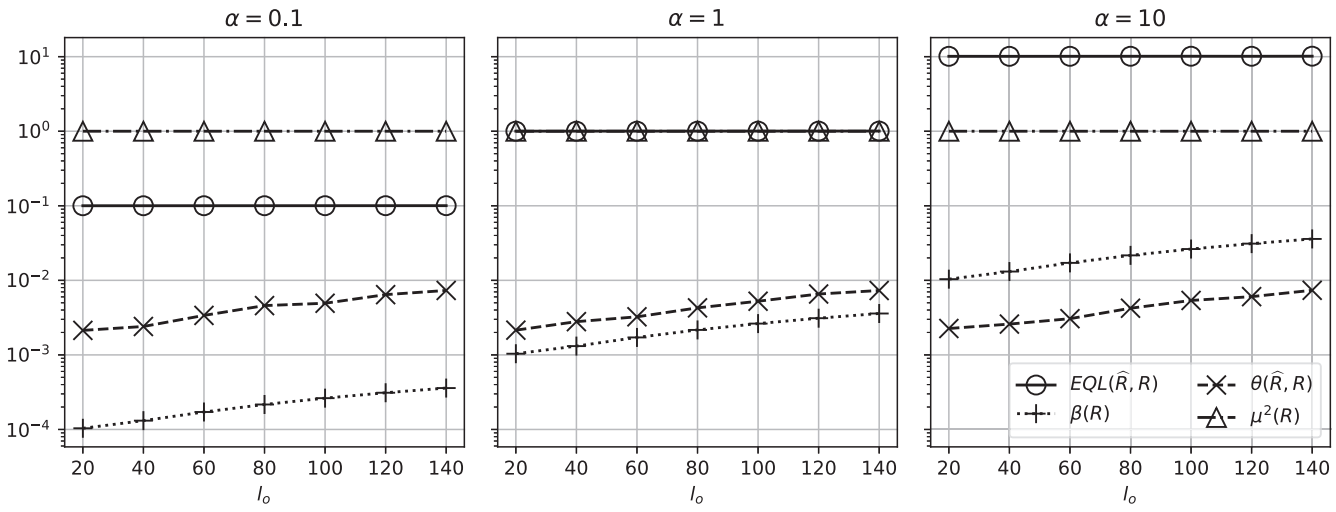

FIGURE 2 As Figure 1, but varying observation-error correlation length-scale (l_o).

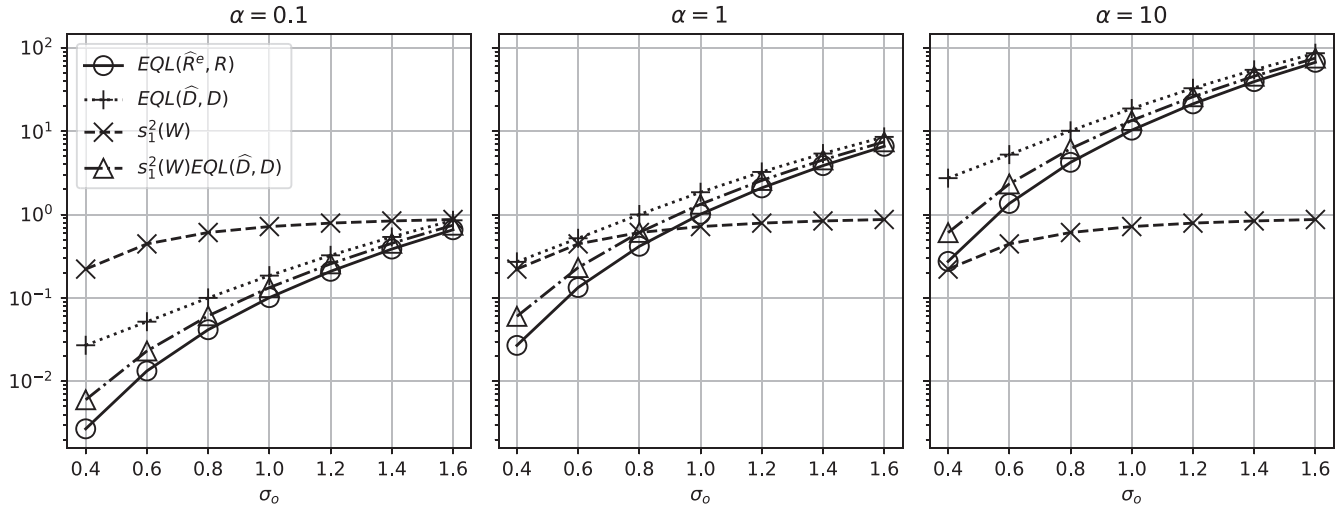

FIGURE 3 Sampling error with the Desroziers et al. method using exact assumed error statistics EQL($\hat{\mathbf{R}}^{\mathrm{e}}, \mathbf{R}$), direct sampling error EQL($\hat{\mathbf{D}}, \mathbf{D}$), the square of the largest singular value of $\mathbf{W}$, $s_1^2(\mathbf{W})$, and the upper bound of EQL($\hat{\mathbf{R}}^{\mathrm{e}}, \mathbf{R}$) given by the product of EQL($\hat{\mathbf{D}}, \mathbf{D}$) and $s_1^2(\mathbf{W})$ (Theorem 3) as a function of observation-error standard deviation (σ_{o}) for three different ratios (α) of the number of observations to sample size. The y-axis is plotted using a log scale.

exact value of EQL($\hat{\mathbf{R}}^{\mathrm{e}}, \mathbf{R}$) and its upper bound is

$$\sum_{i=1}^{m}\sum_{j=1}^{m}\left|(s_1(\mathbf{W}) - s_i(\mathbf{W}))z_{ij}\right|^2, \tag{56}$$

where z_{ij} denotes an element of the matrix $\mathbf{Z}$, which is an orthogonal transformation of ($\hat{\mathbf{D}} - \mathbf{D}$) defined in Appendix C. Equation (56) suggests that the tightness of the bound depends on the difference between the largest singular value and the other singular values of the matrix $\mathbf{W}$, and the size of z_{ij}. For instance, if the singular-value spectrum is flat, or if z_{ij} is small, then we can expect a tight upper bound.

The increase in the upper bound of EQL($\hat{\mathbf{R}}^{\mathrm{e}}, \mathbf{R}$) with varying σ_{o} is a result of the increase in EQL($\hat{\mathbf{D}}, \mathbf{D}$) and $s_1^2(\mathbf{W})$. The term EQL($\hat{\mathbf{D}}, \mathbf{D}$) measures direct sampling errors. As the innovation covariance matrix, $\mathbf{D}$, is formed using the matrices $\mathbf{B}$ and $\mathbf{R}$ (Equation 14), the size of its elements increases with σ_{o}. Then, using the results on direct sampling error in Section 8.2.1, we can expect EQL($\hat{\mathbf{D}}, \mathbf{D}$) to increase with σ_{o}. The increase in $s_1^2(\mathbf{W})$ can be explained by the following equation:

$$\tau_k(\mathbf{W}) = \frac{\tau_k(\mathbf{R})}{\tau_k(\mathbf{R}) + \tau_k(\mathbf{H}\mathbf{B}\mathbf{H}^{\top})}, \tag{57}$$

where $\tau_k(\cdot)$ denotes the eigenvalue of a matrix that is ordered by wavenumber $k = 1, \ldots, m-1$. For symmetric matrices, the singular values are equivalent to the eigenvalues. The notation $\tau_k(\cdot)$ is used to distinguish this case from the notation $\lambda_i(\cdot)$, which denotes the eigenvalue of a matrix ordered by size. Equation (57) holds if the matrices $\mathbf{R}$ and $\mathbf{H}\mathbf{B}\mathbf{H}^{\top}$ are circulant (see Appendix E for derivation). In our experiments, they are circulant due to the way they are constructed. We know that an increase in σ_{o} increases all eigenvalues of $\mathbf{R}$, which according to Equation (57) also increases all eigenvalues of $\mathbf{W}$. Due to the symmetry of the matrix, the eigenvalues and singular values of $\mathbf{W}$ are equal. Thus, $s_1^2(\mathbf{W})$ increases with σ_{o}.

In contrast to the variation of indirect sampling error, EQL($\hat{\mathbf{R}}^{\mathrm{e}}, \mathbf{R}$), with σ_{o}, EQL($\hat{\mathbf{R}}^{\mathrm{e}}, \mathbf{R}$) does not seem to vary much with the background-error standard deviation (σ_{b}), as shown in Figure 4. We note that in fact EQL($\hat{\mathbf{R}}^{\mathrm{e}}, \mathbf{R}$) increases slightly with σ_{b}; however, this is not clearly visible from Figure 4, as the y-axis is plotted on a logarithmic scale. In comparison, the increase in the upper bound of EQL($\hat{\mathbf{R}}^{\mathrm{e}}, \mathbf{R}$) is more pronounced. The upper bound is given by the product of EQL($\hat{\mathbf{D}}, \mathbf{D}$) and $s_1^2(\mathbf{W})$, where the former is found to increase with σ_{b} and the latter is found to decrease with σ_{b}. From the definition of the matrix $\mathbf{D}$ (Equation 14), an increase in σ_{b} will increase the size of the elements of $\mathbf{D}$. Then, using the results on direct sampling error (Section 8.2.1), we can expect that an increase in σ_{b} will lead to an increase in EQL($\hat{\mathbf{D}}, \mathbf{D}$). The decrease in $s_1^2(\mathbf{W})$ with increasing σ_{b} can be explained well using Equation (57).

8.3.2 | Varying observation and background-error correlation length-scales

Compared with the variation of indirect sampling error, EQL($\hat{\mathbf{R}}^{\mathrm{e}}, \mathbf{R}$), with the observation-error standard deviation

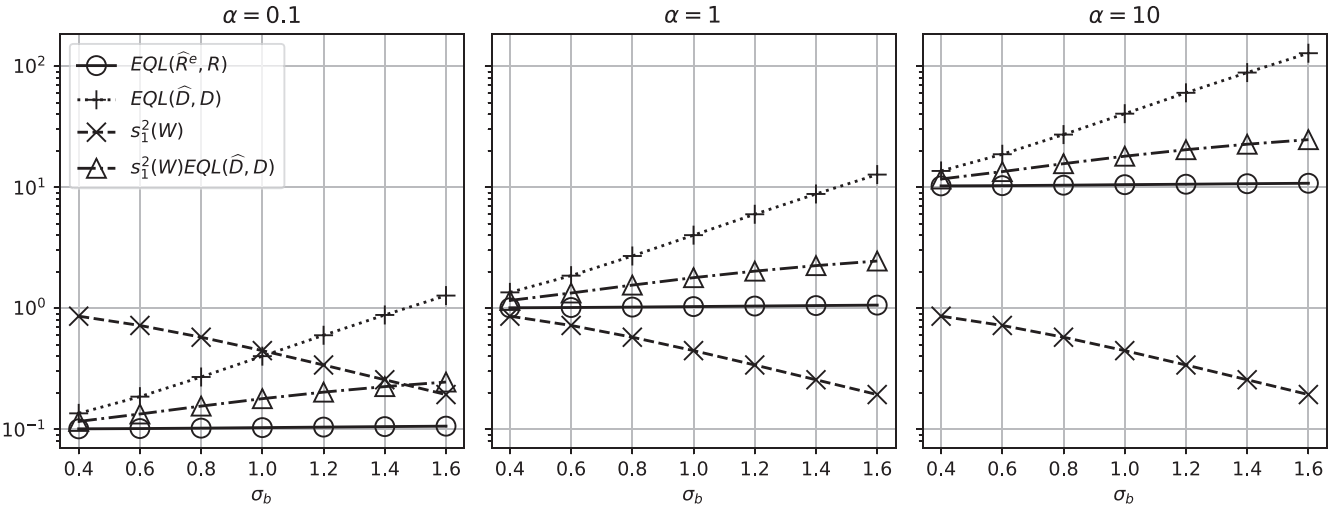

FIGURE 4 As in Figure 3, but for varying background-error standard deviation (σ_b).

(σ_o), the variation of EQL($\widehat{\mathbf{R}}^e, \mathbf{R}$) with the observation and background-error correlation length-scales (l_o and l_b) is very small (Figure 5). The variation of EQL($\widehat{\mathbf{R}}^e, \mathbf{R}$) with l_o and l_b is consistent with the variation of its upper bound, but by a smaller amount. Corollary 1 shows that EQL($\widehat{\mathbf{R}}^e, \mathbf{R}$) with exact assumed error statistics is bounded by the product of EQL($\widehat{\mathbf{D}}, \mathbf{D}$) and $s_1^2(\mathbf{W})$. Since EQL($\widehat{\mathbf{D}}, \mathbf{D}$) measures direct sampling errors (Section 8.2.1) and the size of the elements of $\mathbf{D}$ is determined largely by σ_o and σ_b rather than l_o and l_b, EQL($\widehat{\mathbf{D}}, \mathbf{D}$) should change only slightly as l_o and l_b change. In this experiment, EQL($\widehat{\mathbf{D}}, \mathbf{D}$) is found to vary from 0.1852 to 0.1858 (not shown). Therefore, as shown in Figure 5, changes in the upper bound on EQL($\widehat{\mathbf{R}}^e, \mathbf{R}$) are affected mostly by changes in the square of the largest singular value, $s_1^2(\mathbf{W})$. The change in $s_1^2(\mathbf{W})$ is not always monotonic. For example, when $l_b = 20$ km, $s_1^2(\mathbf{W})$ first decreases and then increases as l_o increases. A similar result is reported in Tabeart *et al.* (2018), where the variation of the condition number of $\mathbf{B}^{-1} + \mathbf{H}^\top \mathbf{R}^{-1} \mathbf{H}$ was not monotonic when changing one of l_o and l_b and fixing the other. We note that these results may not be the case in general.

8.4 | Experiments on sampling error with the Desroziers et al. method (inexact assumed error statistics)

We now show some experimental results for the indirect sampling error with the Desroziers et al. method using inexact assumed error statistics as demonstrated by Theorem 1. We consider a special case in which correlated observation errors are assumed to be uncorrelated in the assimilation. This assumption is sometimes used as a pragmatic strategy in practical data assimilation applications. The experimental setup is as follows: (1) the assumed observation-error covariance matrix ($\widetilde{\mathbf{R}}$) is set as a diagonal matrix; (2) the true observation-error covariance matrix ($\mathbf{R}$) is created using the FOAR correlation function given by Equation (48); and (3) the assumed background-error covariance matrix is exactly the same as the true background-error covariance matrix (i.e., $\widetilde{\mathbf{B}} = \mathbf{B}$), which is generated using the SOAR correlation function given by Equation (50).

Under this experimental design, there are many quantities that we can vary, including the assumed and true error standard deviations and correlation length-scales. Therefore, we choose two particular experiments among them, which we consider to be of more practical interest. Following Waller *et al.* (2016b), we first consider varying the assumed observation-error standard deviation denoted by $\widetilde{\sigma}_o$. This experiment may give us an idea of which size of $\widetilde{\sigma}_o$ we should choose to estimate a correlated $\mathbf{R}$ using the Desroziers et al. method. We then consider varying the true observation-error correlation length-scale (l_o). This experiment shows how large the error caused by the assumption of uncorrelated observation errors can be in terms of different true observation-error correlation length-scales. The parameter values used in these two experiments are listed in Table 1.

8.4.1 | Varying assumed observation-error standard deviation

As shown in Figure 6, the indirect sampling error, EQL($\widehat{\mathbf{R}}^e, \mathbf{R}$), with inexact assumed observation-error

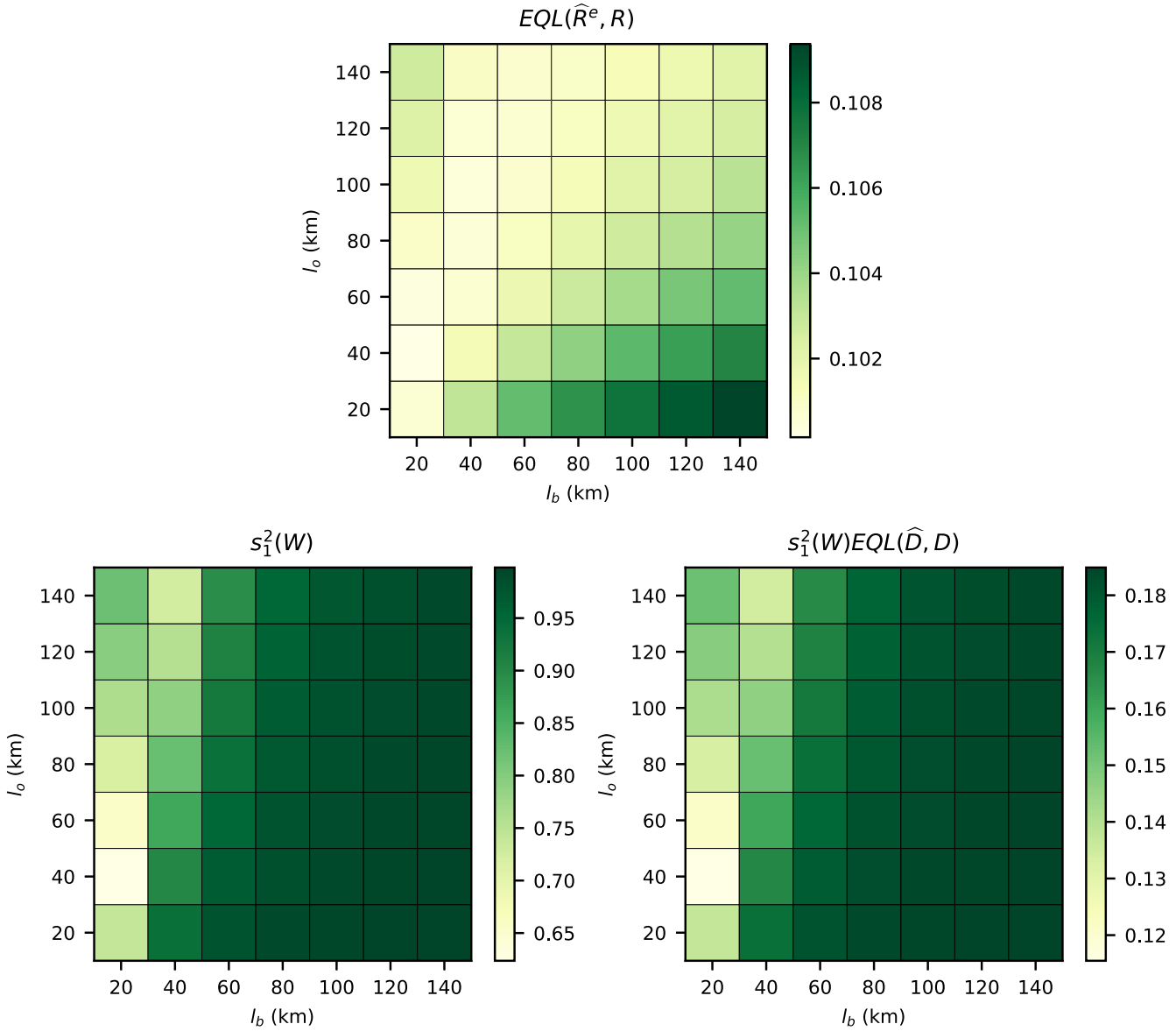

FIGURE 5 Sampling error with the Desroziers et al. method using exact assumed error statistics, EQL($\widehat{\mathbf{R}}^{\mathrm{e}}, \mathbf{R}$), the square of the largest singular value of $\mathbf{W}$, $s_1^2(\mathbf{W})$, and the upper bound of EQL($\widehat{\mathbf{R}}^{\mathrm{e}}, \mathbf{R}$) given by the product of EQL($\widehat{\mathbf{D}}, \mathbf{D}$) and $s_1^2(\mathbf{W})$ (Corollary 1) as a function of observation-error correlation length-scales (l_{o}) and background-error correlation length-scales (l_{b}). [Colour figure can be viewed at wileyonlinelibrary.com]

statistics first decreases and then increases as the assumed observation-error standard deviation ($\widetilde{\sigma}_{\mathrm{o}}$) increases. This can be explained by the variation of the three terms that determine the size of EQL($\widehat{\mathbf{R}}^{\mathrm{e}}, \mathbf{R}$) (see Theorem 1). The first of these terms, EQL($\widehat{\mathbf{R}}^{\mathrm{e}}, \mathbf{R}^{\mathrm{e}}$), is found to increase with $\widetilde{\sigma}_{\mathrm{o}}$ (Figure 6). (Note that EQL($\widehat{\mathbf{R}}^{\mathrm{e}}, \mathbf{R}^{\mathrm{e}}$) measures the indirect sampling error of $\widehat{\mathbf{R}}^{\mathrm{e}}$ with respect to $\mathbf{R}^{\mathrm{e}}$ rather than $\mathbf{R}$). Based on Theorem 3, this term is bounded by the product of EQL($\widehat{\mathbf{D}}, \mathbf{D}$) (direct sampling error in the estimate of the innovation covariance) and $s_1^2(\widetilde{\mathbf{W}})$ (the square of the largest singular value), where EQL($\widehat{\mathbf{D}}, \mathbf{D}$) is only dependent on the exact error statistics and thus does not vary with $\widetilde{\sigma}_{\mathrm{o}}$, and $s_1^2(\widetilde{\mathbf{W}})$ should increase with $\widetilde{\sigma}_{\mathrm{o}}$ following the results in Section 8.3.1. Therefore, the upper bound of EQL($\widehat{\mathbf{R}}^{\mathrm{e}}, \mathbf{R}^{\mathrm{e}}$) should increase as $\widetilde{\sigma}_{\mathrm{o}}$ becomes larger. If EQL($\widehat{\mathbf{R}}^{\mathrm{e}}, \mathbf{R}^{\mathrm{e}}$) follows its upper bound, then we can expect it to increase with $\widetilde{\sigma}_{\mathrm{o}}$ as well.

The term $\frac{1}{m}\|\mathbf{R}^{\mathrm{e}} - \mathbf{R}\|_{\mathrm{F}}^2$ is the second term that determines EQL($\widehat{\mathbf{R}}^{\mathrm{e}}, \mathbf{R}$), and it measures the difference between the estimated and true observation-error covariance matrices. This term is invariant to sample size and is found to first decrease and then increase as $\widetilde{\sigma}_{\mathrm{o}}$ increases. This result agrees with the theoretical findings of Waller *et al.* (2016b, eq. (25)).

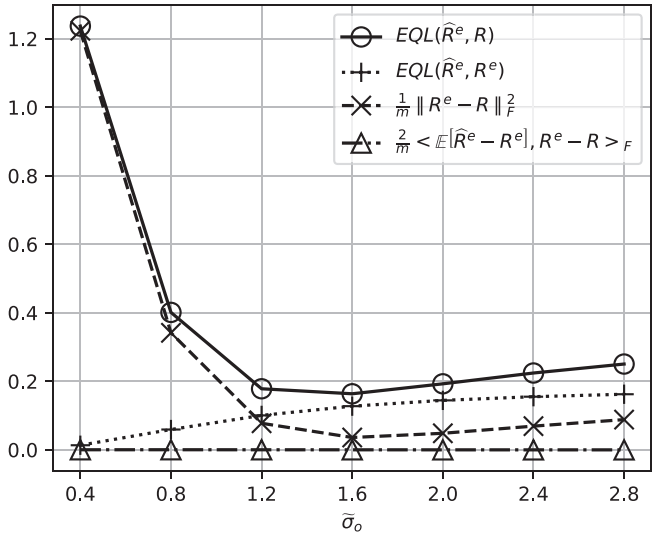

FIGURE 6 Sampling error with the Desroziers et al. method using inexact assumed observation-error statistics, EQL($\widehat{\mathbf{R}}^{\mathrm{e}}, \mathbf{R}$), and the three terms on the right-hand side of Equation (30) as a function of the assumed observation-error standard deviation ($\widetilde{\sigma}_{\mathrm{o}}$).

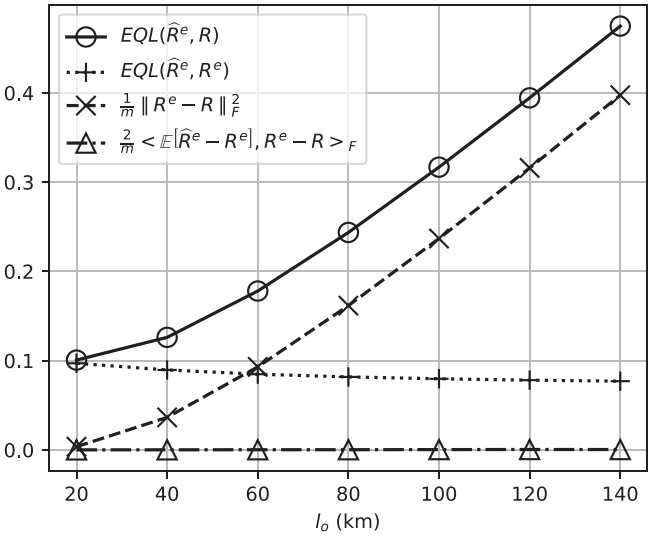

FIGURE 7 As in Figure 6, but for varying observation-error correlation length-scale (l_{o}).

The term $\frac{2}{m}\langle\mathbb{E}\left[\widehat{\mathbf{R}}^{\mathrm{e}} - \mathbf{R}^{\mathrm{e}}\right], \mathbf{R}^{\mathrm{e}} - \mathbf{R}\rangle_{\mathrm{F}}$ is the last of the terms that determines EQL($\widehat{\mathbf{R}}^{\mathrm{e}}, \mathbf{R}$), which is of the order of $10^{-5} \sim 10^{-4}$ in Figure 6. Therefore, this term has very small influence on the size of EQL($\widehat{\mathbf{R}}^{\mathrm{e}}, \mathbf{R}$) in this experiment. However, we note that $\frac{2}{m}\langle\mathbb{E}\left[\widehat{\mathbf{R}}^{\mathrm{e}} - \mathbf{R}^{\mathrm{e}}\right], \mathbf{R}^{\mathrm{e}} - \mathbf{R}\rangle_{\mathrm{F}}$ may be larger and non-negligible under some circumstances. For instance, a larger ratio (α) of the number of observations to sample size will increase $\mathbb{E}\left[\widehat{\mathbf{R}}^{\mathrm{e}} - \mathbf{R}^{\mathrm{e}}\right]$ and thus $\frac{2}{m}\langle\mathbb{E}\left[\widehat{\mathbf{R}}^{\mathrm{e}} - \mathbf{R}^{\mathrm{e}}\right], \mathbf{R}^{\mathrm{e}} - \mathbf{R}\rangle_{\mathrm{F}}$.

Our result implies that the optimal value of $\widetilde{\sigma}_{\mathrm{o}}$ that gives the smallest indirect sampling error, EQL($\widehat{\mathbf{R}}^{\mathrm{e}}, \mathbf{R}$), might be slightly smaller if sampling error is taken into account than if no sampling error is considered. This happens if the amount of increase in EQL($\widehat{\mathbf{R}}^{\mathrm{e}}, \mathbf{R}^{\mathrm{e}}$) is larger than the amount of decrease in $\frac{1}{m}\|\mathbf{R}^{\mathrm{e}} - \mathbf{R}\|_{\mathrm{F}}^2$ as $\widetilde{\sigma}_{\mathrm{o}}$ approaches its optimal value. However, to avoid overfitting, we do not recommend setting $\widetilde{\sigma}_{\mathrm{o}}$ too low in systems with real data.

8.4.2 | Varying true observation-error correlation length-scale

The indirect sampling error, EQL($\widehat{\mathbf{R}}^{\mathrm{e}}, \mathbf{R}$), with inexact assumed observation-error statistics is found to increase when increasing the true observation-error correlation length-scale (l_{o}; Figure 7). To explain this, we shall look at the variation of the three terms that determine the size of EQL($\widehat{\mathbf{R}}^{\mathrm{e}}, \mathbf{R}$) (see Theorem 1). As shown in Figure 7, the first term, EQL($\widehat{\mathbf{R}}^{\mathrm{e}}, \mathbf{R}^{\mathrm{e}}$), decreases slightly with l_{o}, the second term, $\frac{1}{m}\|\mathbf{R}^{\mathrm{e}} - \mathbf{R}\|_{\mathrm{F}}^2$, increases rapidly with l_{o}, and the last term, $\frac{2}{m}\langle\mathbb{E}\left[\widehat{\mathbf{R}}^{\mathrm{e}} - \mathbf{R}^{\mathrm{e}}\right], \mathbf{R}^{\mathrm{e}} - \mathbf{R}\rangle_{\mathrm{F}}$, is of the order of 10^{-5}–10^{-4}. Therefore, when varying l_{o}, the change in EQL($\widehat{\mathbf{R}}^{\mathrm{e}}, \mathbf{R}$) mainly follows the change in $\frac{1}{m}\|\mathbf{R}^{\mathrm{e}} - \mathbf{R}\|_{\mathrm{F}}^2$, because it has a much larger variation than the other two terms. The term $\frac{1}{m}\|\mathbf{R}^{\mathrm{e}} - \mathbf{R}\|_{\mathrm{F}}^2$ measures the difference between the assumed and true observation-error covariance matrices. Because our assumed observation-error covariance matrix is diagonal and the true observation-error covariance is created using the FOAR correlation function with correlation length-scale l_{o} (Equation 48), the difference between the two matrices increases as l_{o} increases.

8.5 | The cross-sectional dispersion of sample eigenvalues

We provide graphical illustrations for Theorem 4 in this section. The experimental design is similar to those in Section 8.3 with exact assumed statistics and those in Section 8.4 with inexact assumed statistics. Figure 8 shows the cross-sectional dispersion of sample eigenvalues in the cases of direct and indirect sampling with exact assumed error statistics as a function of the ratio (α) of the number of observations to sample size. The cross-sectional dispersion of sample eigenvalues is defined as the dispersion of sample eigenvalues around the mean of true eigenvalues (Equation 38). Equations (40) and (41) show that, in the two cases considered in Figure 8, the cross-sectional dispersion of sample eigenvalues should decrease as the sampling error decreases, and if the sampling error is zero then the cross-sectional dispersion of sample eigenvalues

is equal to the spread of the true eigenvalues. This is consistent with the results shown in Figure 8, in which the difference between the cross-sectional dispersion of sample eigenvalues and the spread of the true eigenvalues increases as the ratio $\alpha = m/N$ increases. A larger α means a larger sampling error.

Figure 9 shows the cross-sectional dispersion of sample eigenvalues in the case of indirect sampling with inexact assumed error statistics as a function of α. As shown by Equation (43), an extra Frobenius inner-product term appears in this case and, as a result, the cross-sectional dispersion of sample eigenvalues does not necessarily approach the spread of the true eigenvalues as α decreases. Figure 9 shows that, when $\widetilde{\sigma}_o = 1$, the Frobenius inner-product term is negative and the cross-sectional dispersion of sample eigenvalues approaches a value smaller than the spread of the true eigenvalues as α decreases. However, when $\widetilde{\sigma}_o = 4$, the Frobenius inner-product term becomes positive and the cross-sectional dispersion of sample eigenvalues approaches a value greater than the spread of the true eigenvalues as α decreases. These results indicate that, when using the indirect sampling approach with inexact assumed error statistics, the cross-sectional dispersion of sample eigenvalues may be greater or smaller than the spread of true eigenvalues, depending on the true and assumed error statistics. Figure 9 also indicates that if α is too large then the main influencing factor in the eigenvalue dispersion is the sampling error, while if α is sufficiently small then the main influencing factor is the error due to inexact assumed statistics.

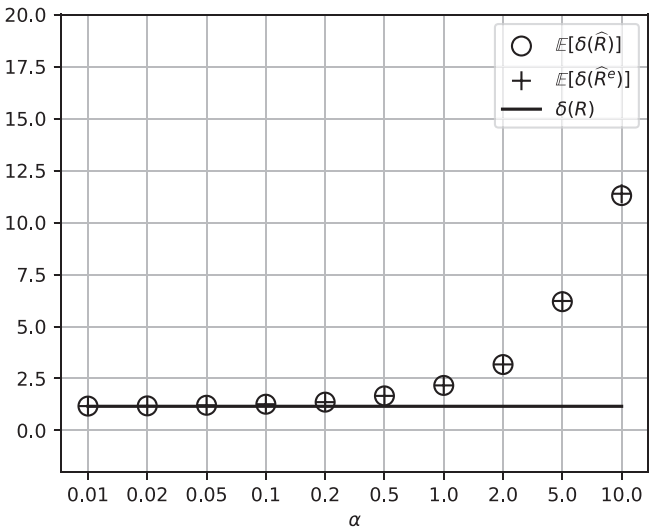

FIGURE 8 The cross-sectional dispersion of sample eigenvalues in the cases of direct sampling ($\mathbb{E}[\delta(\widehat{\mathbf{R}})]$) and indirect sampling with exact assumed error statistics ($\mathbb{E}[\delta(\widehat{\mathbf{R}}^e)]$) as the ratio ($\alpha$) of the number of observations to sample size increases. The symbol $\delta(\mathbf{R})$ denotes the spread of true eigenvalues. For details of the quantities plotted see Theorem 4.

8.5.1 | The spectra of true and sample eigenvalues

We provide some further interpretation of the cross-sectional dispersion of sample eigenvalues. In the case of direct sampling, if the cross-sectional dispersion of sample eigenvalues is larger than the spread of true

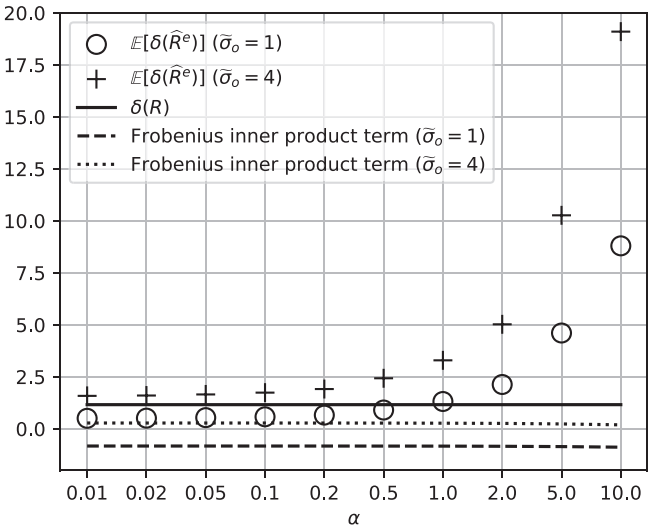

FIGURE 9 The cross-sectional dispersion of sample eigenvalues in the case of indirect sampling with inexact assumed error statistics ($\mathbb{E}[\delta(\widehat{\mathbf{R}}^e)]$) as the ratio ($\alpha$) of the number of observations to sample size increases. The symbol $\delta(\mathbf{R})$ denotes the spread of true eigenvalues. The symbol $\widetilde{\sigma}_o$ denotes the assumed observation-error standard deviation. The Frobenius inner-product term is defined in Theorem 4.

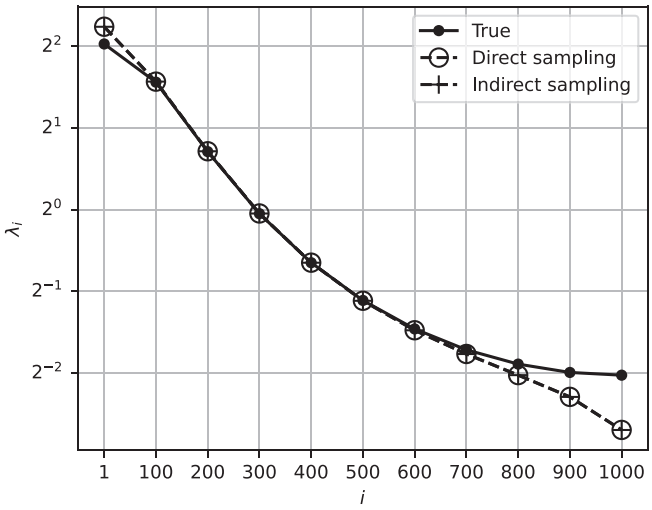

FIGURE 10 The eigenvalues of the true observation-error covariance matrix, the sample covariance matrix obtained using the direct sampling approach, and the sample covariance matrix obtained using the indirect sampling approach with exact assumed error statistics.

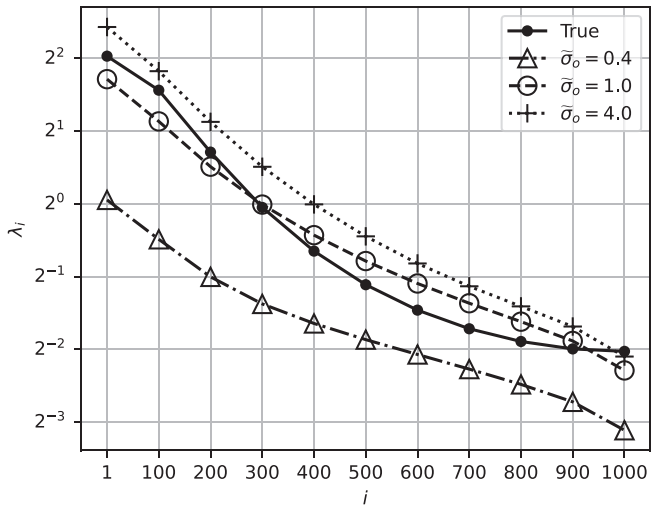

FIGURE 11 The eigenvalues of the true observation-error covariance matrix and the sample covariance matrices obtained using the indirect sampling approach with inexact assumed observation-error standard deviations ($\widetilde{\sigma}_o$).

eigenvalues, then the largest sample eigenvalues are larger than the corresponding true eigenvalues and the smallest eigenvalues are smaller than the corresponding true eigenvalues (e.g., Ledoit & Wolf, 2004). In the case of indirect sampling with exact assumed error statistics, the same result is expected, since Equations (40) and (41) are equivalent. For an illustration of the sample and true eigenvalues in these two cases see Figure 10.

In the case of indirect sampling with inexact assumed error statistics, the cross-sectional dispersion of sample eigenvalues may be larger or smaller than the spread of true eigenvalues, and we observe three circumstances for the difference between the sample and true eigenvalues in Figure 11.

- All sample eigenvalues are *smaller* than the corresponding true eigenvalues.
- The largest and smallest sample eigenvalues are *smaller* than the corresponding true eigenvalues, while the moderate eigenvalues are *larger* than the corresponding eigenvalues.
- Most sample eigenvalues are *larger* than the corresponding true eigenvalues, except for the smallest sample eigenvalues.

The first circumstance arises when the assumed observation-error standard deviation, $\widetilde{\sigma}_o$, has the smallest value considered. When $\widetilde{\sigma}_o$ is increased to 1.0, the second circumstance appears. When we further increase $\widetilde{\sigma}_o$ to 4.0, the third circumstance occurs. We have also carried out experiments with larger values of $\widetilde{\sigma}_o$ (not shown). Even when $\widetilde{\sigma}_o = 100$, a few of the smallest eigenvalues are still smaller than the corresponding true eigenvalues. We also note that in the first two circumstances the cross-sectional dispersion of sample eigenvalues is smaller than the spread of true eigenvalues, while in the last circumstance the cross-sectional dispersion of sample eigenvalues is larger than the spread of true eigenvalues.

For circulant matrices, the effect of varying $\widetilde{\sigma}_o$ on the eigenvalues of the matrix $\mathbf{R}^e$ can be explained by

$$\tau_k(\mathbf{R}^e) = \frac{\tau_k(\widetilde{\mathbf{R}})}{\tau_k(\widetilde{\mathbf{R}}) + \tau_k(\mathbf{H}\widetilde{\mathbf{B}}\mathbf{H}^\top)}\left[\tau_k(\mathbf{R}) + \tau_k(\mathbf{H}\mathbf{B}\mathbf{H}^\top)\right], \quad (58)$$

which is proved in Appendix E. A similar equation is shown in Waller *et al.* (2016b) but with a slightly different formulation. We know that an increase in $\widetilde{\sigma}_o$ will lead to an increase in all eigenvalues of $\widetilde{\mathbf{R}}$, which, based on Equation (58), will increase all eigenvalues of $\mathbf{R}^e$ further. As the previous results show (Figure 9), the sample eigenvalues (eigenvalues of $\widehat{\mathbf{R}}^e$) can be fairly close to the eigenvalues of $\mathbf{R}^e$ as long as α is small enough.

8.5.2 | Implications for matrix modification and reconditioning

Our results may provide some guidance for the modification of the observation-error covariance matrices estimated using the Desroziers et al. approach. Multiplicative variance inflation is used primarily to compensate for the effects of ignoring observation-error correlations, which increase the matrix elements by multiplying each element by a given factor (Bormann *et al.*, 2016). This is equivalent to multiplying all the eigenvalues of the matrix by the same factor. Therefore, if all the sample eigenvalues are less than the corresponding true eigenvalues, the multiplicative variance inflation method can bring the sample eigenvalues closer to the true eigenvalues. The underestimation of the true eigenvalues may happen when the observation errors that are actually correlated are assumed to be uncorrelated in data assimilation and the assumed observation-error variance is too small (for an example see Figure 11). A shortcoming of the multiplicative variance inflation method is that it cannot improve the condition number of the estimated observation-error covariance matrices. A larger condition number may slow down the convergence of the least-squared minimisation in variational data assimilation. The RR and ME methods are two existing methods that can be used to reduce the condition number of any covariance matrix (e.g., Tabeart *et al.*, 2020b). The RR method increases all eigenvalues of the matrix by adding an equal amount to them, while the ME method amends the eigenvalues below a certain value to a given value while leaving the rest unchanged. If we apply these approaches to the observation-error covariance matrices estimated using the Desroziers et al. method, they can also reduce the difference between the

sample and true eigenvalues if the sample eigenvalues are smaller than the corresponding true eigenvalues (for an example see Figure 11).

In practice, it might be difficult to predict whether the sample eigenvalues estimated using the Desroziers et al. method are likely to be greater or less than the true eigenvalues. The difference between $\tau_k(\mathbf{R})$ and $\tau_k(\widehat{\mathbf{R}}^{\mathrm{e}})$ is a combination of the difference between $\tau_k(\mathbf{R})$ and $\tau_k(\mathbf{R}^{\mathrm{e}})$ and the difference between $\tau_k(\mathbf{R}^{\mathrm{e}})$ and $\tau_k(\widehat{\mathbf{R}}^{\mathrm{e}})$. In the case of circulant matrices, the difference between $\tau_k(\mathbf{R})$ and $\tau_k(\mathbf{R}^{\mathrm{e}})$ is (using Equation 58)

$$\tau_k(\mathbf{R}) - \tau_k(\mathbf{R}^{\mathrm{e}}) = \frac{\tau_k(\mathbf{R})\tau_k(\widetilde{\mathbf{H}}\widetilde{\mathbf{B}}\mathbf{H}^{\top}) - \tau_k(\widetilde{\mathbf{R}})\tau_k(\mathbf{H}\mathbf{B}\mathbf{H}^{\top})}{\tau_k(\widetilde{\mathbf{R}}) + \tau_k(\widetilde{\mathbf{H}}\widetilde{\mathbf{B}}\mathbf{H}^{\top})}, \tag{59}$$

which shows that the difference between $\tau_k(\mathbf{R})$ and $\tau_k(\mathbf{R}^{\mathrm{e}})$ is dependent on the assumed and true background and observation-error statistics as well as the observation operator. Although Equation (59) is derived in the case of circulant matrices, there is some evidence from Waller *et al.* (2016c) suggesting that the qualitative results for circulant matrices are still applicable to non-circulant matrices in an operational setting.

In addition to the difference between $\tau_k(\mathbf{R})$ and $\tau_k(\mathbf{R}^{\mathrm{e}})$ given by Equation (59), the difference between $\tau_k(\mathbf{R}^{\mathrm{e}})$ and $\tau_k(\widehat{\mathbf{R}}^{\mathrm{e}})$, namely sampling error, is also affected by the assumed and true error statistics and the observation operator. Therefore, in practical applications, expert opinion on the values of the quantities such as true and assumed observation and background-error standard deviations is required to conjecture whether $\tau_k(\widehat{\mathbf{R}}^{\mathrm{e}})$ is greater or less than $\tau_k(\mathbf{R})$.

9 | CONCLUSION

In this article, we developed new theorems that can be used to analyse sampling errors in the estimation of observation-error covariance matrices using the Desroziers et al. approach (Desroziers *et al.*, 2005). The Desroziers et al. method is an indirect sampling approach, as it does not sample directly from the observation-error characteristics, but uses samples of O−A and O−B differences to estimate the observation-error statistics indirectly. These samples are readily available in most data assimilation systems, making the Desroziers et al. approach widely adopted in practical applications to estimate error correlations for remote-sensing observations such as geostationary satellite data and Doppler radar wind. Although this method produces noisy estimates that have to be reconditioned for operational use, to the best of our knowledge, no systematic investigation of the sampling error with this method has been carried out so far, which brings us to the purpose of this article.

Previously, Waller *et al.* (2016b) investigated the accuracy of the Desroziers et al. method when using different assumed observation and background-error variances and correlation length-scales. Waller *et al.* (2016b) showed that, when correlated observation errors are assumed to be uncorrelated, the Desroziers et al. method will underestimate the observation-error variance and correlation length-scale. However, in Waller *et al.* (2016b) the estimated observation-error covariance matrices were not calculated from samples of the O−A and O−B residuals, and hence the statistical nature of the Desroziers et al. method has not been examined. This work complements the work by Waller *et al.* (2016b) by taking the sampling error into account.

In this study, the expected quadratic loss defined in Equation (20) is used to measure the sampling error with the Desroziers et al. method, which is written as $\mathrm{EQL}(\widehat{\mathbf{R}}^{\mathrm{e}}, \mathbf{R}) = \frac{1}{m}\mathbb{E}\left[\|\widehat{\mathbf{R}}^{\mathrm{e}} - \mathbf{R}\|_{\mathrm{F}}^2\right]$, where $\mathbf{R}$ is the true observation-error covariance matrix and $\widehat{\mathbf{R}}^{\mathrm{e}}$ is the observation-error covariance matrix estimated using finite samples of O−A and O−B residuals (Equation 19). We find that $\mathrm{EQL}(\widehat{\mathbf{R}}^{\mathrm{e}}, \mathbf{R})$ is determined by three terms: an indirect sampling-error term, a misspecification-error term, and a Frobenius inner-product term (Theorem 1). The indirect sampling-error term is written as $\mathrm{EQL}(\widehat{\mathbf{R}}^{\mathrm{e}}, \mathbf{R}^{\mathrm{e}})$, which measures the indirect sampling error in the estimation of $\mathbf{R}^{\mathrm{e}}$ using indirect samples, that is, the samples of O−A and O−B residuals. The matrix $\mathbf{R}^{\mathrm{e}}$ is the observation-error covariance matrix estimated via the Desroziers et al. method, but in exact arithmetic (Equation 18), so that it does not contain any sampling error. The size of $\mathrm{EQL}(\widehat{\mathbf{R}}^{\mathrm{e}}, \mathbf{R}^{\mathrm{e}})$ is bounded by the product of $s_1^2(\widetilde{\mathbf{W}})$ and $\mathrm{EQL}(\widehat{\mathbf{D}}, \mathbf{D})$ (Theorem 3). The term $s_1^2(\widetilde{\mathbf{W}})$ is the square of the largest singular value of $\widetilde{\mathbf{W}} = \widetilde{\mathbf{R}}(\widetilde{\mathbf{H}}\widetilde{\mathbf{B}}\mathbf{H}^{\top} + \widetilde{\mathbf{R}})^{-1}$, which has an upper bound given in Equation (35) and can be easily calculated in the case of circulant matrices (Equation 57). The matrix $\mathbf{D}$ is the innovation covariance matrix (Equation 14) and $\widehat{\mathbf{D}}$ is a sample covariance matrix of $\mathbf{D}$ (Equation 15). The term $\mathrm{EQL}(\widehat{\mathbf{D}}, \mathbf{D})$ measures the direct sampling error in the estimation of $\mathbf{D}$ using samples that are drawn directly from $\mathbf{D}$. Direct sampling errors can be analysed using previous work by Ledoit and Wolf (2004). The misspecification-error term $\frac{1}{m}\|\mathbf{R}^{\mathrm{e}} - \mathbf{R}\|_{\mathrm{F}}^2$ describes the error of the Desroziers et al. method caused by the misspecification of assumed observation and background-error statistics. Its size can be estimated using previous work by Waller *et al.* (2016b). The Frobenius inner-product term, $\frac{2}{m}\langle\mathbb{E}\left[\widehat{\mathbf{R}}^{\mathrm{e}} - \mathbf{R}^{\mathrm{e}}\right], \mathbf{R}^{\mathrm{e}} - \mathbf{R}\rangle_{\mathrm{F}}$, is the last term that determines $\mathrm{EQL}(\widehat{\mathbf{R}}^{\mathrm{e}}, \mathbf{R})$, which is found to be very small if the sample size is sufficiently large (for examples see Figures 6 and 7). Since this term may be hard to compute in practice, we further provide an upper bound

for EQL($\hat{\mathbf{R}}^{e}, \mathbf{R}$) (Theorem 2). This upper bound can be estimated using the terms EQL($\hat{\mathbf{R}}^{e}, \mathbf{R}^{e}$) and $\frac{1}{m}\|\mathbf{R}^{e} - \mathbf{R}\|_{F}^{2}$.

Our theoretical analysis and numerical results showed that, when using O−A and O−B statistics to estimate observation-error covariance matrices, a larger sampling error is expected if the true observation-error standard deviation is larger, while the other true error statistics, including background-error standard deviation and observation and background-error correlation length-scales, have a relatively small effect on the sampling error. This suggests that we may consider using different ratios of the number of observations to sample size for different types of observations. If an observation type is expected to have a large observation-error standard deviation, then we may need a large sample size to ensure accuracy, whereas if the error standard deviation of an observation type is expected to be small then we may use a small sample size for efficiency. In addition, if we do not have any prior knowledge of the true observation-error standard deviation and the estimated value is quite large, then we may consider increasing the sample size to see if the estimate changes significantly. Since we have shown that the sampling error increases as the assumed observation-error standard deviation increases, the reader might be tempted to reduce the assumed observation-error standard deviation to reduce the sampling error. However, if the assumed observation-error standard deviation is too small, this will lead to overfitting of the observational data in the assimilation. This is likely to lead to poor analyses and spurious results (Dance, 2020). Moreover, the sampling error may be much smaller than the error due to the misspecification of the background and observation-error statistics. Therefore, we should set the assumed observation-error standard deviation as accurately as possible.

We further investigated the difference between the eigenvalues of the estimated and true observation-error covariance matrices. We started by extending the results of Ledoit and Wolf (2004) on cross-sectional dispersion of sample eigenvalues to a more general case (Theorem 4). The cross-sectional dispersion of sample eigenvalues is defined as the spread of the sample eigenvalues around the mean of the true eigenvalues (Equation 38). Ledoit and Wolf (2004) showed that, in the case of direct sampling, the sample eigenvalues are more dispersed around the mean of the true eigenvalues than the true eigenvalues themselves. This means that the largest sample eigenvalues are larger than the corresponding true eigenvalues and the smallest sample eigenvalues are smaller than the corresponding true eigenvalues. However, when using the Desroziers et al. method to estimate the true observation-error covariance matrix, the cross-sectional dispersion of the sample eigenvalues (eigenvalues of $\hat{\mathbf{R}}^{e}$) may be smaller or larger than the spread of the true eigenvalues (eigenvalues of $\mathbf{R}$). In the case of indirect sampling, the difference between the sample and true eigenvalues is determined by the sampling error as well as the error due to inexact assumed error statistics. These two errors are affected by a variety of quantities, including the assumed and true background and observation-error covariances and the observation operator. As a consequence, expert opinion on the values of these quantities is needed to anticipate which sample eigenvalues are likely to be larger than the true eigenvalues and which sample eigenvalues are likely to be smaller than the true eigenvalues.

Our analysis can be used to evaluate sampling errors in estimating observation-error covariance matrices using the Desroziers et al. method. Our approach provides information on how sampling error and estimated eigenvalues are expected to change under particular variations in assumed and true observation and background-error statistics. Our theoretical results are general. Our numerical experiments are carried out with circulant matrices. However, the results obtained may still be qualitatively useful for inferring what would happen in real-data experiments with non-circulant matrices.

ACKNOWLEDGEMENTS

G. Hu was funded in part by the Engineering and Physical Sciences Research Council, UK EPSRC DARE project (EP/P002331/1), NERC NCEO, and the Met Office. S. L. Dance was funded in part by the Engineering and Physical Sciences Research Council, UK EPSRC DARE project, (EP/P002331/1) and NERC NCEO. We thank three anonymous reviewers for their valuable comments.

CONFLICT OF INTEREST STATEMENT

We declare we have no competing interests.

DATA AVAILABILITY STATEMENT

The data used to create the figures in this article were generated by a simple numerical experiment, which is described in Section 8.1. The experiment was conducted using Python. We also include the specific Python functions used in the main text. The Python code is available on request from the corresponding author.

ORCID

Guannan Hu https://orcid.org/0000-0003-4305-3658
Sarah L. Dance https://orcid.org/0000-0003-1690-3338

REFERENCES

Anderson, E., Fisher, M., Munro, R. & McNally, A. (2000) Diagnosis of background errors for radiances and other observable quantities in a variational data assimilation scheme, and the

explanation of a case of poor convergence. *Quarterly Journal of the Royal Meteorological Society*, 126(565), 1455–1472. Available from: https://doi.org/10.1002/qj.49712656512

Ballard, S.P., Li, Z., Simonin, D. & Caron, J.-F. (2016) Performance of 4D-Var NWP-based nowcasting of precipitation at the met Office for summer 2012. *Quarterly Journal of the Royal Meteorological Society*, 142(694), 472–487. Available from: https://doi.org/10.1002/qj.2665

Bathmann, K. (2018) Justification for estimating observation-error covariances with the Desroziers diagnostic. *Quarterly Journal of the Royal Meteorological Society*, 144(715), 1965–1974. Available from: https://doi.org/10.1002/qj.3395

Bédard, J. & Buehner, M. (2020) A practical assimilation approach to extract smaller-scale information from observations with spatially correlated errors: an idealized study. *Quarterly Journal of the Royal Meteorological Society*, 146(726), 468–482. Available from: https://doi.org/10.1002/qj.3687

Bernstein, D.S. (2009) *Matrix mathematics: theory, facts, and formulas*, 2nd edition. Princeton, NJ: Princeton University Press. Available from: https://doi.org/10.1515/9781400833344

Bickel, P.J. & Levina, E. (2008) Regularized estimation of large covariance matrices. *The Annals of Statistics*, 36(1), 199–227. Available from: https://doi.org/10.1214/009053607000000758

Bormann, N., Bonavita, M., Dragani, R., Eresmaa, R., Matricardi, M. & McNally, A. (2016) Enhancing the impact of IASI observations through an updated observation-error covariance matrix. *Quarterly Journal of the Royal Meteorological Society*, 142(697), 1767–1780.

Bouttier, F. & Courtier, P. (2002) *Data assimilation concepts and methods March 1999. Meteorological training course lecture series*, Vol. 718. Reading UK: ECMWF, p. 59.

Campbell, W.F., Satterfield, E.A., Ruston, B. & Baker, N.L. (2017) Accounting for correlated observation error in a dual-formulation 4D variational data assimilation system. *Monthly Weather Review*, 145(3), 1019–1032.

Chun, H.-W., Eresmaa, R., McNally, A.P., Bormann, N. & Matricardi, M. (2015) A physically-based observation-error covariance matrix for IASI. In: *The 20th International TOVS Study Conference (ITSC-20)*. Lake Geneva, WI: International TOVS Working Group. Available from: https://cimss.ssec.wisc.edu/itwg/itsc/itsc20/program/

Cordoba, M., Dance, S.L., Kelly, G.A., Nichols, N.K. & Waller, J.A. (2017) Diagnosing atmospheric motion vector observation errors for an operational high-resolution data assimilation system. *Quarterly Journal of the Royal Meteorological Society*, 143(702), 333–341. Available from: https://doi.org/10.1002/qj.2925

Dance, S.L. (2020) Estimating observation errors: diagnostics, possibilities, and pitfalls. In: *Presentation at the Virtual Event: ECMWF/EUMETSAT NWP SAF Workshop on the Treatment of Random and Systematic Errors in Satellite Data Assimilation for NWP, November 04, 2020*. https://events.ecmwf.int/event/170/contributions/1534/attachments/946/1652/Errors-WS-Dance.pdf

Dance, S.L., Ballard, S.P., Bannister, R.N., Clark, P., Cloke, H.L., Darlington, T. et al. (2019) Improvements in forecasting intense rainfall: results from the FRANC (forecasting rainfall exploiting new data assimilation techniques and novel observations of convection) project. *Atmosphere*, 10(3), 125. Available from: https://doi.org/10.3390/atmos10030125, https://www.mdpi.com/2073-4433/10/3/125

Desroziers, G., Berre, L., Chapnik, B. & Poli, P. (2005) Diagnosis of observation, background and analysis-error statistics in observation space. *Quarterly Journal of the Royal Meteorological Society*, 131(613), 3385–3396.

Dey, D.K. & Srinivasan, C. (1985) Estimation of a covariance matrix under Stein's loss. *The Annals of Statistics*, 13(4), 1581–1591. Available from: https://doi.org/10.1214/aos/1176349756

Field, A. (2018) *Discovering statistics using IBM SPSS statistics*, 5th edition. Burswood, WA: Sage edge.

Fowler, A.M., Dance, S.L. & Waller, J.A. (2018) On the interaction of observation and prior error correlations in data assimilation. *Quarterly Journal of the Royal Meteorological Society*, 144(710), 48–62. Available from: https://doi.org/10.1002/qj.3183

Fujita, T., Seko, H., Kawabata, T., Ikuta, Y., Sawada, K., Hotta, D. et al. (2020) *Variational data assimilation with spatial and temporal observation error correlations of Doppler radar radial winds*. Working Group on Numerical Experimentation. Report.

Furrer, R. & Bengtsson, T. (2007) Estimation of high-dimensional prior and posterior covariance matrices in Kalman filter variants. *Journal of Multivariate Analysis*, 98(2), 227–255. Available from: https://doi.org/10.1016/j.jmva.2006.08.003, https://www.sciencedirect.com/science/article/pii/S0047259X06001187

Geer, A.J. (2019) Correlated observation error models for assimilating all-sky infrared radiances. *Atmospheric Measurement Techniques*, 12(7), 3629–3657. Available from: https://doi.org/10.5194/amt-12-3629-2019, https://amt.copernicus.org/articles/12/3629/2019/

Golub, G.H. & Van Loan, C.F. (1996) *Matrix computations*. Baltimore, MD: Johns Hopkins University Press.

Gray, R.M. (2006) Toeplitz and circulant matrices: a review. *Foundations and Trends® in Communications and Information Theory*, 2(3), 155–239. Available from: https://doi.org/10.1561/0100000006

Guillet, O., Weaver, A.T., Vasseur, X., Michel, Y., Gratton, S. & Gürol, S. (2019) Modelling spatially correlated observation errors in variational data assimilation using a diffusion operator on an unstructured mesh. *Quarterly Journal of the Royal Meteorological Society*, 145(722), 1947–1967. Available from: https://doi.org/10.1002/qj.3537

Haben, S.A. (2011) *Conditioning and preconditioning of the minimisation problem in variational data assimilation*. PhD thesis. University of Reading. https://www.reading.ac.uk/maths-and-stats/publications/theses-and-dissertations/mathematics-phd-theses

Haff, L.R. (1980) Empirical Bayes estimation of the multivariate normal covariance matrix. *The Annals of Statistics*, 8(3), 586–597. Available from: https://doi.org/10.1214/aos/1176345010

Hamill, T.M., Whitaker, J.S. & Snyder, C. (2001) Distance-dependent filtering of background error covariance estimates in an ensemble Kalman filter. *Monthly Weather Review*, 129(11), 2776–2790.

Haramoto, H., Matsumoto, M., Nishimura, T., Panneton, F. & L'Ecuyer, P. (2008) Efficient jump ahead for F2-linear random number generators. *INFORMS Journal on Computing*, 20(3), 385–390.

Harris, C.R., Millman, K.J., van der Walt, S.J., Gommers, R., Virtanen, P., Cournapeau, D. et al. (2020) Array programming with NumPy. *Nature*, 585(7825), 357–362. Available from: https://doi.org/10.1038/s41586-020-2649-2

Healy, S. & White, A. (2005) Use of discrete Fourier transforms in the 1D-Var retrieval problem. *Quarterly Journal of the Royal Meteorological Society*, 131(605), 63–72.

Higham, N.J. (2002) Computing the nearest correlation matrix–a problem from finance. *IMA Journal of Numerical Analysis*, 22(3), 329–343. Available from: https://doi.org/10.1093/imanum/22.3.329

Horn, R.A. & Johnson, C.R. (1991) *Topics in matrix analysis*. Cambridge, UK: Cambridge University Press. Available from: https://doi.org/10.1017/CBO9780511840371

Houtekamer, P.L. & Mitchell, H.L. (2001) A sequential ensemble Kalman filter for atmospheric data assimilation. *Monthly Weather Review*, 129(1), 123–137.

Hu, G. & Dance, S.L. (2021) Efficient computation of matrix-vector products with full observation weighting matrices in data assimilation. *Quarterly Journal of the Royal Meteorological Society*, 147, 4101–4121. Available from: https://doi.org/10.1002/qj.4170

Hu, G., Dance, S.L., Bannister, R.N., Chipilski, H.G., Guillet, O., Macpherson, B. et al. (2022) Progress, challenges, and future steps in data assimilation for convection-permitting numerical weather prediction: report on the virtual meeting held on 10 and 12 November 2021. *Atmospheric Science Letters*, 24(1), e1130. Available from: https://doi.org/10.1002/asl.1130

Huber, P.J. (2004) *Robust statistics*. New York: John Wiley & Sons. Available from: https://doi.org/10.1002/9780470434697

Janjić, T., Bormann, N., Bocquet, M., Carton, J.A., Cohn, S.E., Dance, S.L. et al. (2018) On the representation error in data assimilation. *Quarterly Journal of the Royal Meteorological Society*, 144(713), 1257–1278. Available from: https://doi.org/10.1002/qj.3130

Jensen, J.L.W.V. (1906) Sur les fonctions convexes et les inégalités entre les valeurs moyennes. *Acta Mathematica*, 30, 175–193. Available from: https://doi.org/10.1007/BF02418571

Jeong, J. & Jun, M. (2015) Covariance models on the surface of a sphere: when does it matter? *Stat*, 4(1), 167–182. Available from: https://doi.org/10.1002/sta4.84

Ledoit, O. & Wolf, M. (2004) A well-conditioned estimator for large-dimensional covariance matrices. *Journal of Multivariate Analysis*, 88(2), 365–411. Available from: https://doi.org/10.1016/S0047-259X(03)00096-4, https://www.sciencedirect.com/science/article/pii/S0047259X03000964

Liu, Z.-Q. & Rabier, F. (2003) The potential of high-density observations for numerical weather prediction: a study with simulated observations. *Quarterly Journal of the Royal Meteorological Society*, 129(594), 3013–3035.

Ménard, R. (2016) Error covariance estimation methods based on analysis residuals: theoretical foundation and convergence properties derived from simplified observation networks. *Quarterly Journal of the Royal Meteorological Society*, 142(694), 257–273. Available from: https://doi.org/10.1002/qj.2650

Michel, Y. (2018) Revisiting Fisher's approach to the handling of horizontal spatial correlations of observation errors in a variational framework. *Quarterly Journal of the Royal Meteorological Society*, 144(716), 2011–2025. Available from: https://doi.org/10.1002/qj.3249

Mirza, A.K., Dance, S.L., Rooney, G.G., Simonin, D., Stone, E.K. & Waller, J.A. (2021) Comparing diagnosed observation uncertainties with independent estimates: a case study using aircraft-based observations and a convection-permitting data assimilation system. *Atmospheric Science Letters*, 22(5), el01029. Available from: https://doi.org/10.1002/asl.1029

Nichols, N.K. (2010) Mathematical concepts of data assimilation. In: Lahoz, W., Khattatov, B. & Menard, R. (Eds.) *Data assimilation: making sense of observations*. Berlin: Springer, pp. 13–39. Available from: https://doi.org/10.1007/978-3-540-74703-1_2

Rainwater, S., Bishop, C.H. & Campbell, W.F. (2015) The benefits of correlated observation errors for small scales. *Quarterly Journal of the Royal Meteorological Society*, 141(693), 3439–3445. Available from: https://doi.org/10.1002/qj.2582

Satterfield, E.A., Waller, J.A., Kuhl, D.D., Hodyss, D., Hoppel, K.W., Eckermann, S.D. et al. (2022) Statistical parameter estimation for observation error modelling: application to meteor radars. In: Park, S.K. & Xu, L. (Eds.) *Data assimilation for atmospheric, oceanic and hydrologic applications*, Vol. IV. Cham: Springer International Publishing, pp. 185–213. Available from: https://doi.org/10.1007/978-3-030-77722-7_8

Simonin, D., Waller, J.A., Ballard, S.P., Dance, S.L. & Nichols, N.K. (2019) A pragmatic strategy for implementing spatially correlated observation errors in an operational system: an application to Doppler radial winds. *Quarterly Journal of the Royal Meteorological Society*, 145(723), 2772–2790.

Stewart, L.M. (2010) *Correlated observation errors in data assimilation*. PhD thesis. University of Reading.

Stewart, L.M., Dance, S. & Nichols, N. (2008) Correlated observation errors in data assimilation. *International Journal for Numerical Methods in Fluids*, 56(8), 1521–1527.

Stewart, L.M., Dance, S.L. & Nichols, N.K. (2013) Data assimilation with correlated observation errors: experiments with a 1-D shallow water model. *Tellus A: Dynamic Meteorology and Oceanography*, 65(1), 19546.

Stewart, L.M., Dance, S.L., Nichols, N.K., Eyre, J.R. & Cameron, J. (2014) Estimating interchannel observation-error correlations for IASI radiance data in the met Office system. *Quarterly Journal of the Royal Meteorological Society*, 140(681), 1236–1244. Available from: https://doi.org/10.1002/qj.2211

Tabeart, J.M. (2019) *On the treatment of correlated observation errors in data assimilation*. PhD thesis. University of Reading. https://www.reading.ac.uk/maths-and-stats/publications/theses-and-dissertations/mathematics-phd-theses

Tabeart, J.M., Dance, S.L., Haben, S.A., Lawless, A.S., Nichols, N.K. & Waller, J.A. (2018) The conditioning of least-squares problems in variational data assimilation. *Numerical Linear Algebra with Applications*, 25(5), e2165.

Tabeart, J.M., Dance, S.L., Lawless, A.S., Migliorini, S., Nichols, N.K., Smith, F. et al. (2020a) The impact of using reconditioned correlated observation-error covariance matrices in the met Office 1D-Var system. *Quarterly Journal of the Royal Meteorological Society*, 146(728), 1372–1390.

Tabeart, J.M., Dance, S.L., Lawless, A.S., Nichols, N.K. & Waller, J.A. (2020b) Improving the condition number of estimated covariance matrices. *Tellus A: Dynamic Meteorology and Oceanography*, 72(1), 1–19.

Tabeart, J.M., Dance, S.L., Lawless, A.S., Nichols, N.K. & Waller, J.A. (2021) New bounds on the condition number of the Hessian of the preconditioned variational data assimilation problem. *Numerical Linear Algebra with Applications*, 29, e2405. Available from: https://doi.org/10.1002/nla.2405

Tandeo, P., Ailliot, P., Bocquet, M., Carrassi, A., Miyoshi, T., Pulido, M. et al. (2020) A review of innovation-based methods to jointly estimate model and observation error

covariance matrices in ensemble data assimilation. *Monthly Weather Review*, 148(10), 3973–3994. Available from: https://doi.org/10.1175/MWR-D-19-0240.1, https://journals.ametsoc.org/view/journals/mwre/148/10/mwrD190240.xml

Waller, J.A., Ballard, S.P., Dance, S.L., Kelly, G., Nichols, N.K. & Simonin, D. (2016a) Diagnosing horizontal and inter-channel observation error correlations for SEVIRI observations using observation-minus-background and observation-minus-analysis statistics. *Remote Sensing*, 8(7), 581. Available from: https://doi.org/10.3390/rs8070581, https://www.mdpi.com/2072-4292/8/7/581

Waller, J.A., Bauernschubert, E., Dance, S.L., Nichols, N.K., Potthast, R. & Simonin, D. (2019) Observation error statistics for Doppler radar radial wind superobservations assimilated into the DWD COSMO-KENDA system. *Monthly Weather Review*, 147(9), 3351–3364. Available from: https://doi.org/10.1175/MWR-D-19-0104.1, https://journals.ametsoc.org/view/journals/mwre/147/9/mwr-d-19-0104.1.xml

Waller, J.A., Dance, S.L. & Nichols, N.K. (2016b) Theoretical insight into diagnosing observation error correlations using observation-minus-background and observation-minus-analysis statistics. *Quarterly Journal of the Royal Meteorological Society*, 142(694), 418–431. Available from: https://doi.org/10.1002/qj.2661

Waller, J.A., Dance, S.L. & Nichols, N.K. (2017) On diagnosing observation-error statistics with local ensemble data assimilation. *Quarterly Journal of the Royal Meteorological Society*, 143(708), 2677–2686. Available from: https://doi.org/10.1002/qj.3117

Waller, J.A., Simonin, D., Dance, S.L., Nichols, N.K. & Ballard, S.P. (2016c) Diagnosing observation error correlations for Doppler radar radial winds in the met Office UKV model using observation-minus-background and observation-minus-analysis statistics. *Monthly Weather Review*, 144(10), 3533–3551. Available from: https://doi.org/10.1175/MWR-D-15-0340.1, https://journals.ametsoc.org/view/journals/mwre/144/10/mwr-d-15-0340.1.xml

Weston, P., Bell, W. & Eyre, J. (2014) Accounting for correlated error in the assimilation of high-resolution sounder data. *Quarterly Journal of the Royal Meteorological Society*, 140(685), 2420–2429.

Yaglom, A.M. (1987) *Correlation theory of stationary and related random functions, volume I: basic results*, Vol. 131. Cham: Springer.

Yeh, H.-L., Yang, S.-C., Terasaki, K., Miyoshi, T. & Liou, Y.-C. (2022) Including observation error correlation for ensemble radar radial wind assimilation and its impact on heavy rainfall prediction. *Quarterly Journal of the Royal Meteorological Society*, 148(746), 2254–2281. Available from: https://doi.org/10.1002/qj.4302

How to cite this article: Hu, G. & Dance, S.L. (2024) Sampling and misspecification errors in the estimation of observation-error covariance matrices using observation-minus-background and observation-minus-analysis statistics. *Quarterly Journal of the Royal Meteorological Society*, 1–26. Available from: https://doi.org/10.1002/qj.4750

APPENDIX A. PROOF OF THEOREM 1

We have

$$\begin{aligned}\frac{1}{m}\mathbb{E}\left[\|\widehat{\mathbf{R}}^{\mathrm{e}}-\mathbf{R}\|_{\mathrm{F}}^2\right] &= \frac{1}{m}\mathbb{E}\left[\|\widehat{\mathbf{R}}^{\mathrm{e}}-\mathbf{R}^{\mathrm{e}}+\mathbf{R}^{\mathrm{e}}-\mathbf{R}\|_{\mathrm{F}}^2\right]\\ &= \frac{1}{m}\mathbb{E}\left[\|\widehat{\mathbf{R}}^{\mathrm{e}}-\mathbf{R}^{\mathrm{e}}\|_{\mathrm{F}}^2\right]+\frac{1}{m}\|\mathbf{R}^{\mathrm{e}}-\mathbf{R}\|_{\mathrm{F}}^2\\ &\quad+\frac{2}{m}\mathbb{E}\left[\left\langle\widehat{\mathbf{R}}^{\mathrm{e}}-\mathbf{R}^{\mathrm{e}},\mathbf{R}^{\mathrm{e}}-\mathbf{R}\right\rangle_{\mathrm{F}}\right]\\ &= \frac{1}{m}\mathbb{E}\left[\|\widehat{\mathbf{R}}^{\mathrm{e}}-\mathbf{R}^{\mathrm{e}}\|_{\mathrm{F}}^2\right]+\frac{1}{m}\|\mathbf{R}^{\mathrm{e}}-\mathbf{R}\|_{\mathrm{F}}^2\\ &\quad+\frac{2}{m}\left\langle\mathbb{E}\left[\widehat{\mathbf{R}}^{\mathrm{e}}-\mathbf{R}^{\mathrm{e}}\right],\mathbf{R}^{\mathrm{e}}-\mathbf{R}\right\rangle_{\mathrm{F}},\end{aligned}\tag{A1}$$

as required.

APPENDIX B. PROOF OF THEOREM 2

Using the triangle inequality, we obtain

$$\begin{aligned}\|\widehat{\mathbf{R}}^{\mathrm{e}}-\mathbf{R}\|_{\mathrm{F}} &= \|\widehat{\mathbf{R}}^{\mathrm{e}}-\mathbf{R}^{\mathrm{e}}+\mathbf{R}^{\mathrm{e}}-\mathbf{R}\|_{\mathrm{F}}\\ &\leqslant \|\widehat{\mathbf{R}}^{\mathrm{e}}-\mathbf{R}^{\mathrm{e}}\|_{\mathrm{F}}+\|\mathbf{R}^{\mathrm{e}}-\mathbf{R}\|_{\mathrm{F}}.\end{aligned}\tag{B1}$$

Then we have

$$\begin{aligned}\frac{1}{m}\mathbb{E}\left[\|\widehat{\mathbf{R}}^{\mathrm{e}}-\mathbf{R}\|_{\mathrm{F}}^2\right] &\leqslant \frac{1}{m}\mathbb{E}\left[\left(\|\widehat{\mathbf{R}}^{\mathrm{e}}-\mathbf{R}^{\mathrm{e}}\|_{\mathrm{F}}+\|\mathbf{R}^{\mathrm{e}}-\mathbf{R}\|_{\mathrm{F}}\right)^2\right]\\ &\leqslant \frac{1}{m}\mathbb{E}\left[\|\widehat{\mathbf{R}}^{\mathrm{e}}-\mathbf{R}^{\mathrm{e}}\|_{\mathrm{F}}^2\right]+\frac{1}{m}\|\mathbf{R}^{\mathrm{e}}-\mathbf{R}\|_{\mathrm{F}}^2\\ &\quad+2\|\mathbf{R}^{\mathrm{e}}-\mathbf{R}\|_{\mathrm{F}}\cdot\frac{1}{m}\mathbb{E}\left[\|\widehat{\mathbf{R}}^{\mathrm{e}}-\mathbf{R}^{\mathrm{e}}\|_{\mathrm{F}}\right].\end{aligned}\tag{B2}$$

Then, we use Jensen's inequality (Jensen, 1906):

$$\frac{1}{m}\mathbb{E}\left[\|\widehat{\mathbf{R}}^{\mathrm{e}}-\mathbf{R}^{\mathrm{e}}\|_{\mathrm{F}}\right]\leqslant\sqrt{\frac{1}{m^2}\mathbb{E}\left[\|\widehat{\mathbf{R}}^{\mathrm{e}}-\mathbf{R}^{\mathrm{e}}\|_{\mathrm{F}}^2\right]}.\tag{B3}$$

This completes the proof.

APPENDIX C. PROOF OF THEOREM 3

Let $\widetilde{\mathbf{W}}=\mathbf{V}\mathbf{S}\mathbf{G}^{\top}$ be the singular-value decomposition of a $m\times m$ matrix $\widetilde{\mathbf{W}}$, where $\mathbf{V}\in\mathbb{R}^{m\times m}$ and $\mathbf{G}\in\mathbb{R}^{m\times m}$ are orthogonal matrices and $\mathbf{S}=\mathrm{diag}(s_1(\widetilde{\mathbf{W}}),s_2(\widetilde{\mathbf{W}}),\ldots,s_m(\widetilde{\mathbf{W}}))$ is a diagonal matrix with diagonal elements that are the singular values. Suppose the singular values are arranged in descending order, so that $\max_i|s_i(\widetilde{\mathbf{W}})|=s_1(\widetilde{\mathbf{W}})$. Since the Frobenius norm is unitarily invariant (e.g., Horn & Johnson, 1991, section 5.6), we obtain

$$\|\widetilde{\mathbf{W}}(\widehat{\mathbf{D}}-\mathbf{D})\|_{\mathrm{F}}^2=\|\mathbf{S}\mathbf{G}^{\top}(\widehat{\mathbf{D}}-\mathbf{D})\|_{\mathrm{F}}^2.\tag{C1}$$

Let $\mathbf{Z} = \mathbf{G}^{\top}(\hat{\mathbf{D}} - \mathbf{D})$. Then we have

$$\|\mathbf{SZ}\|_{\mathrm{F}}^2 = \sum_{i=1}^{m}\sum_{j=1}^{m}|s_i(\widetilde{\mathbf{W}})z_{ij}|^2 \leqslant s_1^2(\widetilde{\mathbf{W}})\sum_{i=1}^{m}\sum_{j=1}^{m}|z_{ij}|^2 = s_1^2(\widetilde{\mathbf{W}})\|\mathbf{Z}\|_{\mathrm{F}}^2 = s_1^2(\widetilde{\mathbf{W}})\|\hat{\mathbf{D}} - \mathbf{D}\|_{\mathrm{F}}^2, \tag{C2}$$

as required.

APPENDIX D. PROOF OF THE UPPER BOUND OF S12(W∼)

We begin by noting that $\widetilde{\mathbf{W}} = \widetilde{\mathbf{R}}\widetilde{\mathbf{D}}^{-1}$, where $\widetilde{\mathbf{D}} = \widetilde{\mathbf{R}} + \mathbf{H}\widetilde{\mathbf{B}}\mathbf{H}^{\top}$ is like the innovation covariance matrix defined in Equation (14), but calculated using assumed observation and background-error covariance matrices. The ith singular value of the product of two (real or complex) matrices is smaller than or equal to the product of the largest singular value of the first matrix and the ith singular value of the second matrix, or the product of the ith singular value of the first matrix and the largest singular value of the second matrix (Bernstein, 2009, Proposition 9.6.1; Horn & Johnson, 1991). In particular, for $i = 1$,

$$s_1^2(\widetilde{\mathbf{W}}) \leqslant s_1^2(\widetilde{\mathbf{R}})s_1^2(\widetilde{\mathbf{D}}^{-1}). \tag{D1}$$

We know that, for symmetric matrices, the eigenvalues and singular values are the same, therefore

$$s_1^2(\widetilde{\mathbf{W}}) \leqslant \lambda_1^2(\widetilde{\mathbf{R}})\lambda_1^2(\widetilde{\mathbf{D}}^{-1}). \tag{D2}$$

Then, using the fact that the maximum eigenvalue of a matrix is equal to the reciprocal of the minimum eigenvalue of its inverse, we obtain

$$s_1^2(\widetilde{\mathbf{W}}) \leqslant \left(\frac{\lambda_1(\widetilde{\mathbf{R}})}{\lambda_m(\widetilde{\mathbf{D}})}\right)^2. \tag{D3}$$

Finally, using the fact that the minimum eigenvalue of the sum of two (real or complex) matrices is larger than or equal to the sum of the minimum eigenvalues of these two matrices (Bernstein, 2009, Fact 5.12.2), an upper bound of $s_1^2(\widetilde{\mathbf{W}})$ is provided by

$$s_1^2(\widetilde{\mathbf{W}}) \leqslant \left(\frac{\lambda_1(\widetilde{\mathbf{R}})}{\lambda_m(\widetilde{\mathbf{R}}) + \lambda_m(\mathbf{H}\widetilde{\mathbf{B}}\mathbf{H}^{\top})}\right)^2, \tag{D4}$$

as required.

APPENDIX E. THE SIZE OF $s_1^2(\widetilde{\mathbf{W}})$ IN THE CASE OF CIRCULANT $\widetilde{\mathbf{R}}$ AND $\mathbf{H}\widetilde{\mathbf{B}}\mathbf{H}^{\top}$

We provide a fast way to compute the size of $s_1^2(\widetilde{\mathbf{W}})$, which can be used when the matrices $\widetilde{\mathbf{R}}$ and $\mathbf{H}\widetilde{\mathbf{B}}\mathbf{H}^{\top}$ are circulant. We start with the definition and properties of circulant matrices. A circulant matrix is a matrix where each row is obtained by cyclically shifting the preceding row. For example, an $m \times m$ circulant matrix takes the form

$$\mathbf{C} = \begin{bmatrix} c_0 & c_{m-1} & \cdots & c_2 & c_1 \\ c_1 & c_0 & c_{m-1} & & c_2 \\ \vdots & c_1 & c_0 & \ddots & \vdots \\ c_{m-2} & & \ddots & \ddots & c_{m-1} \\ c_{m-1} & c_{m-2} & \cdots & c_1 & c_0 \end{bmatrix}.$$

Circulant matrices have some useful properties.

Fact 1 (Gray (2006, section 3.2)). The sum and product of two circulant matrices are circulant.

Fact 2 (Gray (2006, section 3.2)). The inverse of a circulant matrix is circulant.

Fact 3 (Gray (2006, section 3.2)). Circulant matrices commute.

Fact 4 (Gray (2006, Theorem 3.1)). The kth eigenvector of any $m \times m$ circulant matrix is

$$\mathbf{u}_k = \left(1, \omega^k, \omega^{2k}, \ldots, \omega^{(m-1)k}\right)^{\top},$$

where $\omega = e^{-2\pi i/m}$ is a primitive mth root of unity and i is the imaginary unit.

Recall that $\widetilde{\mathbf{W}} = \widetilde{\mathbf{R}}(\mathbf{H}\widetilde{\mathbf{B}}\mathbf{H}^{\top} + \widetilde{\mathbf{R}})^{-1}$. If the matrices $\widetilde{\mathbf{R}}$ and $\mathbf{H}\widetilde{\mathbf{B}}\mathbf{H}^{\top}$ are circulant, then their sum is circulant (Fact 1) and the inverse of the sum is also circulant (Fact 2). Thus, the matrix $\widetilde{\mathbf{W}}$, as the product of two circulant matrices, is circulant (Fact 1). We also know that $\widetilde{\mathbf{R}}$ and $(\mathbf{H}\widetilde{\mathbf{B}}\mathbf{H}^{\top} + \widetilde{\mathbf{R}})^{-1}$ are symmetric and they commute (Fact 3). Therefore, their product $\widetilde{\mathbf{W}}$ is also symmetric.

Since the singular value of a symmetric matrix is equivalent to the eigenvalue of that matrix, we have

$$s_1(\widetilde{\mathbf{W}}) = \lambda_1(\widetilde{\mathbf{W}}).$$

Furthermore, as circulant matrices share the same eigenvectors (Fact 4), we can write

$$\tau_k(\widetilde{\mathbf{W}}) = \frac{\tau_k(\widetilde{\mathbf{R}})}{\tau_k(\widetilde{\mathbf{R}}) + \tau_k(\mathbf{H}\widetilde{\mathbf{B}}\mathbf{H}^{\top})},$$

where $k = 0, \ldots, m-1$ is the wavenumber and $\tau_k(\cdot)$ denotes the eigenvalues ordered by wavenumber. We use a different notation here to distinguish the eigenvalues denoted by $\lambda_i(\cdot)$, which are ordered by size from the largest to the smallest. Now the task is to find the wavenumber k' that gives the largest eigenvalue of $\widetilde{\mathbf{W}}$ and then the value of $s_1^2(\widetilde{\mathbf{W}})$ can be calculated by

$$s_1^2(\widetilde{\mathbf{W}}) = \left[\frac{\tau_{k'}(\widetilde{\mathbf{R}})}{\tau_{k'}(\widetilde{\mathbf{R}}) + \tau_{k'}(\mathbf{H}\widetilde{\mathbf{B}}\mathbf{H}^\top)}\right]^2.$$

This allows us to compute $s_1^2(\widetilde{\mathbf{W}})$ directly from $\widetilde{\mathbf{R}}$ and $\mathbf{H}\widetilde{\mathbf{B}}\mathbf{H}^\top$ without forming the matrix $\widetilde{\mathbf{W}}$. The kth eigenvalues of $\widetilde{\mathbf{R}}$ and $\mathbf{H}\widetilde{\mathbf{B}}\mathbf{H}^\top$ can be easily computed using the elements of the first row of each matrix (e.g., Haben, 2011, eqs. (5.25) and (5.26)). In addition, if a circulant matrix has no negative elements, its maximum eigenvalue occurs at $k' = 0$ and is equal to the sum of any row of the matrix (e.g., Haben, 2011, eq. (5.28)). However, in our experiments, the matrix $\widetilde{\mathbf{W}}$ may contain negative elements.

APPENDIX F. PROOF OF THEOREM 4

We may write

$$\begin{aligned}
&\frac{1}{m}\mathbb{E}\left[\|\hat{\mathbf{A}} - \mu(\mathbf{A})\cdot\mathbf{I}\|_{\mathrm{F}}^2\right] \\
&= \frac{1}{m}\mathbb{E}\left[\|\hat{\mathbf{A}} - \mathbf{A} + \mathbf{A} - \mu(\mathbf{A})\cdot\mathbf{I}\|_{\mathrm{F}}^2\right] \\
&= \frac{1}{m}\mathbb{E}\left[\|\hat{\mathbf{A}} - \mathbf{A}\|_{\mathrm{F}}^2\right] + \frac{1}{m}\mathbb{E}\left[\|\mathbf{A} - \mu(\mathbf{A})\cdot\mathbf{I}\|_{\mathrm{F}}^2\right] \\
&\quad + \frac{2}{m}\mathbb{E}\left[\left\langle\hat{\mathbf{A}} - \mathbf{A}, \mathbf{A} - \mu(\mathbf{A})\cdot\mathbf{I}\right\rangle_{\mathrm{F}}\right] \\
&= \frac{1}{m}\mathbb{E}\left[\|\hat{\mathbf{A}} - \mathbf{A}\|_{\mathrm{F}}^2\right] + \frac{1}{m}\|\mathbf{A} - \mu(\mathbf{A})\cdot\mathbf{I}\|_{\mathrm{F}}^2 \\
&\quad + \frac{2}{m}\left\langle\mathbb{E}\left[\hat{\mathbf{A}} - \mathbf{A}\right], \mathbf{A} - \mu(\mathbf{A})\cdot\mathbf{I}\right\rangle_{\mathrm{F}}. \qquad \text{(F1)}
\end{aligned}$$

Then, based on Equations (2) and (4), we can find that the Frobenius norm can be given by trace, $\|\mathbf{A}\|_{\mathrm{F}}^2 = \mathrm{tr}(\mathbf{A}^\top\mathbf{A})$. Using this relationship, the second term of the last line in Equation (F1) can be rewritten as

$$\begin{aligned}
&\frac{1}{m}\|\mathbf{A} - \mu(\mathbf{A})\cdot\mathbf{I}\|_{\mathrm{F}}^2 \\
&= \frac{1}{m}\mathrm{tr}\left[(\mathbf{A} - \mu(\mathbf{A})\cdot\mathbf{I})(\mathbf{A} - \mu(\mathbf{A})\cdot\mathbf{I})^\top\right] \\
&= \frac{1}{m}\left[\mathrm{tr}(\mathbf{A}\mathbf{A}^\top) + \mu^2(\mathbf{A}) - 2\mu(\mathbf{A})\cdot\mathrm{tr}(\mathbf{A})\right]. \qquad \text{(F2)}
\end{aligned}$$

Finally, using the relationship between the trace and eigenvalues given by Equation (5), we can further write

$$\begin{aligned}
&\frac{1}{m}\|\mathbf{A} - \mu(\mathbf{A})\cdot\mathbf{I}\|_{\mathrm{F}}^2 \\
&= \frac{1}{m}\left[\sum_{i=1}^{m}\lambda_i^2(\mathbf{A}) + \mu^2(\mathbf{A}) - 2\mu(\mathbf{A})\sum_{i=1}^{m}\lambda_i(\mathbf{A})\right] \\
&= \frac{1}{m}\sum_{i=1}^{m}(\lambda_i(\mathbf{A}) - \mu(\mathbf{A}))^2. \qquad \text{(F3)}
\end{aligned}$$

This completes the proof.